JAERI-Tech
97-008

HEAT TRANSFER AUGMENTATION FOR HIGH HEAT FLUX REMOVAL IN RIB-ROUGHENED NARROW CHANNELS

March 1997

Md. Shafiqul ISLAM, Ryutaro HINO
Katsuhiro HAGA, Masanori MONDE*
and Yukio SUDO

日本原子力研究所
Japan Atomic Energy Research Institute

本レポートは，日本原子力研究所が不定期に公刊している研究報告書です。
入手の問合わせは，日本原子力研究所研究情報部研究情報課（〒319-11 茨城県那珂郡東海村）あて，お申し越しください。なお，このほかに財団法人原子力弘済会資料センター（〒319-11 茨城県那珂郡東海村日本原子力研究所内）で複写による実費頒布をおこなっております。

This report is issued irregularly.
Inquiries about availability of the reports should be addressed to Research Information Division, Department of Intellectual Resources, Japan Atomic Energy Research Institute, Tokai-mura, Naka-gun, Ibaraki-ken 319-11, Japan.

編集兼発行　日本原子力研究所
印　　刷　日立高速印刷株式会社

Heat Transfer Augmentation for High Heat Flux Removal in Rib-roughened Narrow Channels

Md.Shafiqul ISLAM, Ryutaro HINO, Katsuhiro HAGA
Masanori MONDE * and Yukio SUDO

Department of Advanced Nuclear Heat Technology
Oarai Research Establishment
Japan Atomic Energy Research Institute
Oarai-machi, Higashiibaraki-gun, Ibaraki-ken

(Received January 30,1997)

Heat transfer augmentation in narrow rectangular channels in a target system is a very important method to remove high heat flux up to 12MW/m^2 generated at target plates of a high-intensity proton accelerator of 1.5 GeV and 1 mA with a proton beam power of 1.5 MW. In this report, heat transfer coefficients and friction factors in narrow rectangular channels with one-sided rib-roughened surface were evaluated for fully developed flows in the range of the Reynolds number from 6,000 to 1,00,000; the rib pitch-to-height ratios(p/k)were 10,20 and 30; the rib height-to-equivalent diameter ratios(k/De)were 0.025,0.03 and 0.1 by means of previous existing experimental correlations. The rib-roughened surface augmented heat transfer coefficients approximately 4 times higher than the smooth surface at Re=10,000, p/k=10 and k/De=0.1;friction factors increase around 22 times higher. In this case, higher heat flux up to 12 MW/m^2 could be removed from the rib-roughened surface without flow boiling which induces flow instability; but pressure drop reaches about 1.8 MPa. Correlations obtained by air-flow experiments have showed lower heat transfer performance with the water-flow conditions. The experimental apparatus was proposed for further investigation on heat transfer augmentation in very narrow channels under water-flow conditions. This report presents the evaluation results and an outline of the test appararus.

---

*Saga University

Keywords: Heat Transfer Augmentation, Narrow Rectangular Channels, High Heat Flux, Target System, Heat Transfer Coefficients, Friction Factors, Rib-roughened Surface, Pressure Drop, Evaluation, Experimental Apparatus

高熱流束除去のためのリブ付き狭隘流路の伝熱促進

日本原子力研究所大洗研究所核熱利用研究部
M. S. イスラム・日野竜太郎・羽賀　勝洋
門出　政則*・数土　幸夫

（1997年1月30日受理）

1.5MWの陽子ビームを受けるターゲットでは最高12MW／m²の高熱流速を発生し，それを除去するためにターゲットの冷却材流路である矩形狭隘流路の伝熱促進は極めて重要な工学技術である。本報告では，片面加熱のリブ付き狭隘矩形流路の熱伝達率と摩擦損失係数をレイノルズ数（Re）が6000～100000の範囲の発達した流れについて従来の実験式を用いて評価した。このとき，リブのピッチ（p）と高さ（k）の比（p／k）を10，20，30，また，リブ高さと等価直径（De）の比（k／De）は0.025，0.03，0.1で与えた。リブによって粗面化された伝熱面は，Re＝10000，p／k＝10，k／De＝0.1のとき，リブのない平滑な面よりも熱伝達率が約4倍向上することが示された。このような熱伝達率の向上により，12MW／m²という極めて高い熱流速においても，流動不安定を引き起こす沸騰を生じることなく熱除去が可能なことが分かった。ただし，摩擦損失係数は22倍大きくなるため，1.8MPaの圧力損失を生じることが示された。また，空気流動実験で得られた実験式は水流動実験によるそれよりも低い値を示すことが分かった。そこで，ターゲット冷却と同じ水流動条件下で狭隘矩形流路の伝熱促進をさらに詳細に調べるための試験装置を検討した。本報告では，従来の実験式による評価結果と実験装置の概要について述べる。

大洗研究所：〒311-13　茨城県東茨城郡大洗町成田町新堀3607
＊　佐賀大学

Contents

目　　次

1. Introduction

A compact target with high power-density consisting of solid plates will be used in a spallation neutron source with a high-intensity proton accelerator of 1.5 MW proton-beam power. Then, the target plates generate high heat flux up to 12 MW /m^2. The required heat flux is more than ten times of the conventional heat flux. A forced convection with subcooled water in a very narrow rectangular channel at a moderate velocity is one of promising heat removal methods under such high heat flux conditions [2].

The heat comes from a high-intensity proton accelerator of 1.5 GeV and 1 mA (1.5 MW proton-beam power). Tantalum, Tungsten etc. will be used as the target material. For the solid targets, there will be more than 21 plates with different thickness and coolant passages between the plates. The coolant passage is a rectangular channel with 0.15 cm thick and 9.0 cm in length which were defined at the IPNS upgrade design for a 1MW target station [8]. In the design, surface temperature of the target plate is suppressed below 127℃; water flows at a velocity of more than 13.4 m/s in order to prevent from occuring subcooled boiling and then, saturation temperature of water will be 172℃ at 830 kPa (8.32 bar).

Since high-speed water flow can easily induce flow vibration of plates, water velocity should be decreased as low as possible. From this view point, heat transfer augmentation is useful.

One of the well-known methods for augmenting heat transfer is to roughen the surface using repeated ribs. Then, the ribs which work as turbulent promoters disturb the viscous sublayer of the turbulent boundary layer and create local wall turbulence due to flow separation and reattachment between the ribs, which greatly augment the heat transfer [14].

A good knowledge of the heat transfer distribution on and between the ribs is desirable for improving our understanding of the mechanism by which the ribs actually influence on heat transfer [2].

So, the objective of this work is to focus the feasibilitiy studies of heat transfer performance in a very narrow channel with two-dimensional square-ribs in order to make clear the effectiveness of the high heat flux removal performance by heat transfer augmentation.

In this report, the effects of rib configuration (rib height, rib pitch) and channel

height on the average heat transfer and pressure drop in fully developed flow region will be investigated systematically.

The effects of these parameters on the local heat transfer and pressure drop in developing (entrance) and fully developed regions of rib-roughened channel with three different aspect ratios (0.05, 0.15, 0.25) will be evaluated for the Reynolds number range of 6,000 to 1,00,000; the pitch-to-height ratio varies from 10 to 30 and the rib height-to-channel equivalent diameter ratio varies from 0.025 to 0.10.

2. Heat transfer augmentation

In the moody diagram, it can be seen that roughness increases the friction factor (f), with an asymptotic value of f as a function of the ratio of roughness height (k) to tube diameter (D) at large Reynolds numbers. Some effects on heat transfer would also be expected, because roughness disturbs the viscous sublayer in the turbulent boundary layer by rough protrusions; heat transfer rate can be increased by decreasing thickness of the viscous sublayer. In general, it has been found that artificial roughness does increase the heat transfer; however, it increases the friction factor even more.

One variable in relation to roughness is obviously the ratio of roughness height (k) to tube diameter (D), k/D. Edwards and Sherif noted that to be effective, a roughness element must penetrate the viscous sublayer (y^+=5) and for full effectiveness the roughness height should be larger than the combined viscous sublayer and buffer layer thickness (y^+=40). There is almost no increase in heat transfer for greater heights, but the friction factor continues to increase. Other variable is the ratio of pitch (p) to height (k) for the repeated roughness elements[11].

So, surface roughness is commonly used as an effective approach for augmenting the heat transfer coefficients. Because the improved heat transfer performance by roughened surfaces is at the expense of increased pressure drop, accurate prediction techniques for determining the pressure drop(the friction factor) and heat transfer coefficient (Nusselt number) of rib-roughened surfaces are required in design activities of targets etc. This chapter is concerned with the previous experiments for the prediction of friction factors and heat transfer performance in tubes or channels internally roughened with repeated two-dimensional ribs aligned perpendicular to the flow.

height on the average heat transfer and pressure drop in fully developed flow region will be investigated systematically.

The effects of these parameters on the local heat transfer and pressure drop in developing (entrance) and fully developed regions of rib-roughened channel with three different aspect ratios (0.05, 0.15, 0.25) will be evaluated for the Reynolds number range of 6,000 to 1,00,000; the pitch-to-height ratio varies from 10 to 30 and the rib height-to-channel equivalent diameter ratio varies from 0.025 to 0.10.

2. Heat transfer augmentation

In the moody diagram, it can be seen that roughness increases the friction factor (f), with an asymptotic value of f as a function of the ratio of roughness height (k) to tube diameter (D) at large Reynolds numbers. Some effects on heat transfer would also be expected, because roughness disturbs the viscous sublayer in the turbulent boundary layer by rough protrusions; heat transfer rate can be increased by decreasing thickness of the viscous sublayer. In general, it has been found that artificial roughness does increase the heat transfer; however, it increases the friction factor even more.

One variable in relation to roughness is obviously the ratio of roughness height (k) to tube diameter (D), k/D. Edwards and Sherif noted that to be effective, a roughness element must penetrate the viscous sublayer (y^+=5) and for full effectiveness the roughness height should be larger than the combined viscous sublayer and buffer layer thickness (y^+=40). There is almost no increase in heat transfer for greater heights, but the friction factor continues to increase. Other variable is the ratio of pitch (p) to height (k) for the repeated roughness elements[11].

So, surface roughness is commonly used as an effective approach for augmenting the heat transfer coefficients. Because the improved heat transfer performance by roughened surfaces is at the expense of increased pressure drop, accurate prediction techniques for determining the pressure drop(the friction factor) and heat transfer coefficient (Nusselt number) of rib-roughened surfaces are required in design activities of targets etc. This chapter is concerned with the previous experiments for the prediction of friction factors and heat transfer performance in tubes or channels internally roughened with repeated two-dimensional ribs aligned perpendicular to the flow.

As shown in Fig. 1, the ribs are spaced sufficiently far apart and leeward of the rib separated flow reattaches to the surface before again separating in order to negotiate the next rib. This heat-transfer augmentation mechanism is called the separation and reattachment mechanism [3, 4]. Webb et al. (1971) and Liou and Hwang (1993) provided an extensive set of heat transfer and friction factor data in tubes and rectangular channels with a wide range of rib geometries, respectively. The experimental conditions of these two existing experiments are shown in Table 1-1 and 1-2. These two experimental conditions are discussed to find the similarities between water and air correlations.

In the following subsections, the prediction of friction factors and heat transfer coefficients are discussed from the experimental correlations of Webb et al. and Liou and Hwang.

2.1 Correlations obtained by water-flow experiments and application to narrow channel [13]

Friction factors were determined with air as a working fluid under isothermal flow conditions without heat input, which were evaluated by measurement data of pressure drop across the entire length of the rib-roughened tube. The heat-transfer experiments were carried out with air (Pr=0.71), water (Pr=5.1) and n-butyl alcohol (Pr=21.7) in the range of Reynolds number (Re) from 6,000 to 1,00,000 under constant heat flux conditions. A test section consisted of one smooth tube section and five rough tube sections with rectangular ribs of which pitch-to-height ratios (p/k=10, 20, 40) and rib height-to-hydraulic diameter ratios (k/D_e=0.01 to 0.04). Each rough tube section consisted of two identical copper tubes of 36.83 mm in inner diameter and 1524 mm in length. The test section was heated by electricity.

2.1.1 Friction factor correlation

For the results of rib-roughened surfaces to be most useful, general correlations are required for both the friction factor and heat transfer data which cover a wide range of parameters (k/D_e, Re, p/k). Since Nikuradse found the law of the wall and developed the so-called friction similarity law to correlate the friction data for fully developed turbulent flow in tubes with "sand-grain" roughness, the method has been successfully extended by Webb et al. to correlate the

experimental data of friction factors for turbulent flow in tubes with geometrically similar roughness family. Surfaces which are not geometrically similar will require modifications on relationship between the roughness and heat transfer coefficient found by similarity considerations.

Considering friction factors for geometrically similar roughness, the velocity defect law and the law of the wall similarity are used as basic assumptions. The first of these implies, for turbulent flow in a channel, the existence of a region, away from the immediate vicinity of the wall, where the direct effect of viscosity and roughness on the core flow is negligible.

The velocity defect law is described by the following equation :

$$u_c - u / u^* = 2.5 \ln(R/y) \quad (1)$$

The law of the wall implies the existence of a region close to the wall where the velocity distribution depends on the local conditions, y, ρ, ν, τ and k. The law of the wall similarity is described by the following equation :

$$u /u^* = f (y/k, k^+) \quad (2)$$

Assuming a region of overlap, the velocity defect law and the law of the wall similarity described above are combined to give equation (3) for the turbulence dominated part of the wall region with u_k^+ which is a function of k^+.

$$u /u^* = 2.5 \ln(y/k) + u_k^+(k^+) \quad (3)$$

Based on these analysis, Nikuradse developed the friction similarity law for sand-grain roughness surface by assuming equation (3) which holds approximately over the entire cross section. His data covering a wide range of k/D_e was correlated by equation (4) where k^+ is the roughness Reynolds number [$k^+= k/D_e \, Re(f/2)^{0.5}$]

$$u_k^+ = (2/f)^{1/2} + 2.5 \ln(2k/D_e) + 3.75 \quad (4)$$

Equation (4) is called the friction similarity law. The roughness function $u_k^+(k^+)$ is a general function determined empirically for each type of geometrically similar roughness. The roughness function for Nikuradse's sand-grain roughness has the constant value of 8.48 when k^+ is greater than 70; i.e. in completely rough regime $u_k^+(k^+)$ does not depend on k^+. It is, however, expected to be different values for different geometrical roughness configurations. Based on the "friction similarity law", Webb et al. found a successful friction correlation for turbulent tube flow with repeated-rib

roughness by taking into account of the geometrically non-similar roughness parameter, the p/k ratio, as follows :

$$(2/f)^{1/2} = 2.5 \ln(D_e/2k) - 3.75 + 0.95 (p/k)^{0.53} \quad (5)$$

for $p/k \geqq 10$, $k^+ \geqq 35$, $6 \times 10^3 < Re < 10^5$

The smooth surface friction factor was calculated from the following Swamee-Jain (1976) approximation [12] :

$$f_s = 0.0625 / [\log\{5.74/Re^{0.9}\}]^2 \quad (6)$$

The concept can be extended to correlate the friction factor data for turbulent flow in a very narrow rectangular channel with repeated-rib roughness by taking into account of the geometrically non-similar roughness parameters of p/k, rib shape and one-sided constant heat flux condition. Pressure drop along the test section in fully developed flow can be determined by the following equation :

$$\triangle P = 2 \times (L/D_e) \times \rho \times u_m^2 \times f \quad (7)$$

2.1.2 Heat transfer correlation

Analytical method for predicting the friction factors and heat transfer correlations for turbulent flow over rib-roughened surfaces are not still available because of the complex flow conditions, such as flow separation, reattachment and recirculation which are generated by periodic rib-roughness elements. Semi- empirical correlations for the friction factors and heat transfer coefficients are popular in designing equipments with ribs.

According to the similarity law concept developed by Nikuradse (1950) successfully applied to correlate the friction data for fully developed turbulent flow in tubes with "sand-grain" roughness. Based on a heat-momentum transfer analogy, Dipprey and Sabersky (1963) developed the heat transfer similarity law for fully developed turbulent flow in tubes with "sand-grain" roughness, which is complementary to Nikuradse's friction similarity law. Webb et al. (1971) extended the friction and heat transfer similarity law to correlate the friction and heat transfer data for turbulent flow in tubes with repeated-rib roughness elements.

The similarity law was employed to correlate the friction factors and heat transfer coefficients obtained in experiments with rib-roughened annular tubes

by Dalle Donne and Meyer (1977), with rib-roughened parallel plates by Han et al. (1978), with tubes roughened internally by Gee and Webb (1980) and with rib-roughened square channels by Han et al. (1985). Based on the "heat transfer similarity law", Webb et al. found a successful heat transfer similarity relationship for turbulent flow with repeated-rib roughness. That was correlated with the Stanton number (St) as follows :

$$St=(f/2) / [1+(f/2)^{1/2} \{4.5 (k^+)^{0.28} \times Pr^{0.57} - 0.95(p/k)^{0.53} \}] \quad (8)$$

where $k^+ \geqq 35$, $0.71 < Pr < 37.6$

Webb et al. also correlated the following St for the smooth surface as a reference :

$$St_s=(f_s/2) / [1+9.3(f_s/2)^{1/2} (Pr-1) Pr^{-0.25}] \quad (9)$$

The heat transfer augmentation due to the presence of rib-roughness is often expressed as a ratio of the local heat transfer coefficient for the rib-roughened surface to the local heat transfer coefficient of a smooth surface at the same Reynolds number.

It is therefore, convenient to express the local element Nusselt number (Nu_r) in terms of the smooth surface Nusselt number (Nu_s) multiplied by a rib augmentation factor (E_r).

$$Nu_r = E_r Nu_s \quad (10)$$

In the present analysis, the value of E_r is approximately taken to be 4.

The smooth surface Nusselt number is calculated from the following equation:

$$Nu_s = Re\ Pr\ St_s \quad (11)$$

Another Nusselt number for smooth surface is calculated from the following Dittus-Boelter equation:

$$Nu_s= 0.023\ Re^{0.8}\ Pr^{0.4} \quad (12)$$

This equation is valid for $0.71 < Pr < 100$ and $6 \times 10^3 < Re < 10^5$

The concept described above can be applied to correlate the heat transfer data for turbulent flow in a very narrow rectangular channel with repeated-rib roughness by taking into account the geometrically non-similar roughness parameters of p/k, rib shape, one-sided constant heat flux condition.

2.1.3 Analytical Results and Discussion

(a) Boundary layer thickness [1]

Figure 2 shows the relationship between boundary layer thickness and the Reynolds number for Webb et al.'s experimental condition. It is found that heat transfer augmentation can be realized by protruding the ribs over the viscous sublayer; the ribs disturb the viscous sublayer and create local wall turbulence due to flow separation and reattachment between the ribs, which greatly augment the heat transfer coefficient.

The thickness of the smooth surface viscous sublayer in terms of the inner-region coordinate, y^+ is typically taken to be $y^+ \geqq 5$, for buffer layer regime, $5 \leqq y^+ \leqq 40$ and for turbulent flow regime, $y^+ \geqq 40$. In Webb et al.'s experiments, under water-flow condition, heat transfer was augmented in the region of more than 10,000 of Reynolds number. The rib exists in the buffer layer regime within the Reynolds number 10,000 to 80,000. In our experiments discussed in chap.3, rib height is to set at 0.2mm. Figures 3, 4 and 5 show the relationship between boundary layer thickness and the Reynolds number for different channel heights. From these figures, it can be seen that 0.2 mm rib-height will have high potential to augment heat transfer in a very narrow channel under water-flow condition.

(b) Friction factor and Pressure drop

Figure 6 shows the comparison of friction factor predictions with the data of Webb et al. for the k/D=0.02, w/k=0.52 and varying p/k ratios. The results show the very good agreement with the experiments. Figures 7, 8 and 9 show the friction factor predictions with the Reynolds number for the proposed experiments. These figures indicate the effects of the rib pitch-to-height ratios and channel heights, while holding the rib height at a constant value of k=0.2mm. The friction factor of rib-roughened surface is insensitive to the Reynolds number for fully developed flows though the friction factor of the smooth surface has a relation with the Reynolds number.

Figures 10 and 11 show the comparisons of the friction factor ratio(f/f_s) with the Reynolds number for p/k=10, 20, 30 and channel heights of H=1 and 3 mm. The friction factor ratio increases with the Reynolds number; the friction factor is the highest at p/k=10. On the other hand, the friction factor ratio decreases while the channel height increases. Friction factor at channel height of H=1

mm increases with the rib pitches by factors of 20-39, 9.5-19 and 6-12.3 approximately for p/k=10, 20 and 30 respectively, to the smooth surface in the range of Reynolds number from 6000 to 1,00,000.

This trend is physically reasonable because of increasing blockage of the flow passage by the ribs. As for the effect of the rib height, equation (5) indicates that the friction factor decreases with increasing the rib height (k) for a given rib pitch (p). Figures 8 and 9 show the effects of channel height (H) varying from 3 to 10 mm, under constant rib height and its width.

The friction factors are approximately 5.8-19, 3.2-11.3, 2.1-8.3 times higher than those of the smooth surface for p/k=10, 20, 30 at channel height of H=3 mm : 2.1-5.2, 1.3-3.5, 0.9-2.7 times higher for p/k=10, 20, 30 at channel height of H=10 mm respectively with the same range of Reynolds number.

Figures 12, 13 and 14 show the relationship between water velocity and pressure drop along the test channel. It is seen that pressure drop is very high for smaller channel heights in low velocity region. Pressure drop was calculated for the length of 200 mm under 15℃ of water temperature. Pressure drop for smooth surface is also shown for comparison. The results show that pressure drop is the highest at p/k=10. From the discharge pressure of a pump installed in a test loop described in chap.3, the experiments for the rib-roughened surface should be carried out at low velocity while the experiments can be carried out at moderate high velocity for the smooth surfaces. It is possible to determine the heat transfer coefficients for the smooth and the rib-roughened surfaces in low Reynolds number range (low velocity) below 10,000.

(c) Heat transfer performance

In this section, the calculated Nusselt number, Stanton number and their ratios are discussed with relation to the Reynolds number. Temperature distribution in relation with velocity is also discussed for the feasibility studies of the experiments up to CHF. Effects of rib spacing (p), Reynolds number (Re) and channel heights (H) on heat transfer performance can be looked over.

Figure 15 shows the comparison of Nusselt number predictions with the data of Webb et al. for the k/D=0.02, w/k=0.52 and varying p/k ratios. The agreement is excellent with the experiments. Figure 16 shows the relationship between the Nusselt number and the Reynolds number for the rib-roughened surface in

the range of 6,000 to 1,00,000. The Nusselt number of smooth surface is also shown for comparison. Webb et al. and Dittus-Boelter correlations, equations [11] and [12], are used for calculating the smooth surface heat transfer coefficients. As seen in the figure, there is a little difference between their correlations.

The results also show that the rib-roughened surface for p/k=10, 20, 30 augments heat transfer by 3.6-4.33 times, by 2.8-3.3 times, by 2.4-3 times to the smooth surface. Figure 17 shows the Nusselt number ratio for the rib-roughened and the smooth surface as a function of the Reynolds number for various dimensionless pitches (p/k) in H=1mm. The results show that the Nusselt number ratio decreases with increasing the rib pitches. The reason is that wall turbulence enhanced by the flow separation and reattachment by the ribs and the distance between the reattachment point and the successive rib increases with p/k. The heat transfer augmentation for p/k=30 therefore, is smaller than for p/k=10, 20.

Figures 18, 19 and 20 show the same figures as Figs.16 and 17, which represent the heat transfer performance for channel heights 3 and 10 mm. The Nusselt number ratio shown in Fig.19 in the case of H= 3 mm, is lower than that shown in Fig.17 ; the effect of p/k on the Nusselt number is very small in the case of H=10 mm as shown in Fig.20.

Figure 21 shows the relationship between the Stanton and the Reynolds number. The Stanton number for fully developed turbulent flow in smooth surface is also shown for comparison. As shown in the figure, the Stanton number decreases with increasing the Reynolds number and p/k. The maximum value of the Stanton number occurs at p/k=10. The rib-roughened surface with p/k=30, gives the lowest heat transfer coefficients. The Stanton number of the rib-roughened surface for p/k = 10, 20 and 30 is about 2.5-3.8, 2.2-2.9 and 1.8-2.4, times higher than that of the smooth surface.

Figure 22 shows the relationship between the Stanton number ratio and the Reynolds number. The results show that the Stanton number ratio (heat transfer augmentation) decreases with increasing the Reynolds number. The rib-roughened surface with p/k=10 provides the highest heat transfer augmentation. Figures 23, 24 and 25 show the same figures as Figs.21 and 22 but channel heights are 3 and 10 mm. Highest heat transfer augmentation

can be realized by low channel height. From these figures, the respective channel heights of H=3 and 10 mm, provides the same heat transfer performance. Figures 26 and 27 show the relationship between temperature difference and water velocity for channel heights of H=1 and 3 mm. The Reynolds number is also shown in figures due to directly dependent on velocity. The results show that the temperature difference decreases significantly with increasing velocity for both the smooth and the rib-roughened surfaces.

The incipient boiling temperatures of water at a pressure of 2 MPa and 1 MPa are 182℃ and 151℃ respectively; these are indicated in figures as the temperature difference, $\triangle T_i$.

For the rib-roughened surfaces, boiling does not occur under this condition due to the heat transfer augmentation. But for the smooth surfaces, in very low velocity region, boiling will occur with the expense of high pressure drop. From these figures, it is noticed that the experiments have to carry out at higher velocity with the increase of channel heights and accurate temperature measurements are needed to be done for the rib-roughened surface, specially for p/k=10.

2.2 Correlations obtained by air-flow experiments and application to narrow channel [9,10]

Liou and Hwang carried out their experiments to obtain the friction factor and heat transfer data in a rectangular channels with the ribs of triangular, semicircular and square geometries; rib pitch-to-height ratios (p/k=8, 10, 15, 20), rib height-to-equivalent diameter ratio (k/D_e=0.08), the Reynolds number ranging from 7,800 to 50,000. The experiments carried out with air as the working fluid; the test section consisted of 160 mm in width, 40 mm in height,1200 mm in length and constant heat flux boundary condition. The same correlations have been used for the prediction of friction factor and heat transfer data in the case of one- sided rib-roughened very narrow rectangular channels with one-sided constant heat flux boundary condition.

2.2.1 Friction factor correlation

The friction factor in fully developed channel flow can be determined by measuring the pressure drop across the flow channel and the mass flow rate of

air. The friction factor can then be calculated from :

$$f = \triangle P / (G^2/2\,\rho\, g) \times (D_e/4L) \quad (13)$$

Since the Reynolds number depends on the friction factor for fully developed channel flow with different rib heights and pitches, the effects of the Reynolds number and the rib pitch on the friction factor can be correlated by the following expression :

$$f = b_1\, Re^{b_2} (\,p/k)^{b_3} \quad (14)$$

where the coefficients b_1, b_2, and b_3, depend on the rib geometries and can be determined experimentally. The constants are given in Table 2, for the square rib geometry's according to Liou and Hwang experimental conditions. This correlation has been used for fully developed turbulent flow in a very narrow rectangular channel with one-sided rib-roughened, one-sided constant heat flux boundary condition.

The smooth surface friction factor for fully developed turbulent flow in tubes proposed by Blausius as [5] :

$$f_s = 0.079\, Re^{-0.25} \quad (15)$$

This equation is valid for $6\times10^3 < Re < 10^6$ and can be applied any type of geometry. The smooth surface friction factor for laminar flow can be calculated as:

$$f = K16/Re \quad (16)$$

where K is a constant depending on cross section of geometry.

2.2.2 Heat transfer correlation

The wall similarities based on the roughened channel analysis discussed earlier were employed to correlate the friction and heat transfer performance for fully developed turbulent flow in rectangular channels with two opposite rib-roughened surfaces.

Han (1988) [5, 6, 7] developed friction and heat transfer correlations for fully developed turbulent flow in rectangular channels with two-opposite rib-grooved or rib-roughened surfaces. He applied the friction and heat transfer similarity law for the prediction of friction and heat transfer correlations.

Liou and Hwang (1993) developed correlations of friction factor [equation (14)] and heat transfer from the friction and heat transfer similarity law for different

geometries. Since the Nusselt number depends on the rib height, the rib pitch, and the Reynolds number using these parameters, the correlation can be expressed by the empirical relationship:

$$Nu / Nu_s = a_1 Re^{a_2} (p/k)^{a_3} \quad (17)$$

where the constants a_1, a_2, and a_3 are listed inTable 2, and Nu_s is the Nusselt number of the smooth surface. The well-known correlation developed by Dittus-Boelter can be used for the prediction of Nu_s in the case of air-flow experiments. This correlation is valid for both the air and water. In this section, the main objective is to investigate the feasibility studies whether the air correlations could be used or not for the case of water-flow experiments.

2.2.3 Analytical Results and Discussion

(a) Boundary layer thickness [1]

It can be said that at lower Reynolds number, the turbulence eddies are small in the flow region close to the ribs and that the heat flux is large due to steep temperature gradients, whereas at higher Reynolds number, the turbulent eddies are large in the core flow region and the temperature gradients are small. As the Reynolds number is increased, the acceleration of the flow through the channel is increased and inturn the forced convection is augmented due to thinner boundary layer development on the rib tip at higher Reynolds number.

Figure 28 shows the relationship between the Reynolds number and boundary layer thickness in the case of air-flow experiments carried out by Liou et al.'s.

Figure 29 also shows the relationship between the Reynolds number and boundary layer thickness for the case of proposed experiments discussed in chap. 3 if the experiments were carried out by air in a very narrow channel. The relationship shows for channel height of H=1mm and for more channel heights, it is beyond to describe.

The Reynolds number has been taken $6,000 < Re < 2,00,000$, while the velocity is 47- 157 m/s. The viscous sublayer, buffer and turbulent layers are taken to be $y^+ \leqq 5$, $5 \leqq y^+ \leqq 40$ and $y^+ \geqq 40$, respectively. From both the figures, it is seen that the ribs hold over the buffer layer region. So, the conclusion can be drawn that in the case of air-flow experiments with a very narrow channel, the rib heights should be over the buffer layer region to enhance heat transfer by creating strong turbulence.

(b) Friction factor

Figures 30 and 31 show the relationship between the friction factor and the Reynolds number for air from the empirical correlation [equation (14)] obtained by air-flow experiments. The results show that the friction factor does not influence on the Reynolds number for the channel heights of H=1 and 3 mm, while holding the rib height constant. For p/k=10 provides the highest friction factor compared to other larger p/k cases. These figures basically show the effect of pitch on the friction factor and the Reynolds number for the rib-roughened surfaces compared to the smooth surface.

The friction factors for the rib-roughened surface are approximately 5.3-9.2, 3.4-6.4, 2.6-5.1 times higher than the smooth one in the range of Reynolds number from 1,000 to 40,000 studied. Laminar flow friction factor of the smooth surface is also shown due to clear understanding of transition to turbulent region. It is apparent that for laminar flow the surface roughness has no effect on the friction factor; for turbulent flow, however, the friction factor is at a minimum for a smooth surface. The laminar flow is confined to the region Re < 2,000. The transitional turbulence occurs in the region 2,000 < Re < 8,000. The fully turbulent flow occurs in the region Re > 8,000. Velocity is shown due to ease understanding of flow characteristics.

Channel heights do not influence any significant effect on friction factor and the Reynolds number in the case of air-flow experiments, while in the water-flow experiments, the channel heights play an important role on friction factor and heat transfer performance. Figures 32 and 33 show the relationship between the friction factor and the Reynolds number for water from the empirical correlations obtained by air-flow experiments. The results show that these two figures indicate the same figures as Figs. 30 and 31. The difference is that the water properties are used instead of air properties. As friction factor does not depend on fluid properties, so, the two figures 32 and 33 show the same figures as figs.30 and 31

(c) Heat transfer performance

Many correlations are available for predicting the heat transfer performances in the case of air-flow experiments. Liou and Hwang, Han et al., and Berger et al., are one of them. Liou and Hwang's experimental condition is taken as a reference for comparing the heat transfer performances.

According to equation [17], Figs. 34, 35, 36 and 37 show the relationship between the Nusselt number and the Reynolds number. Figures 34 and 35 show the relationship for air-flow channel with 1 and 3 mm of height which was calculated with the empirical correlations obtained by air-flow experiments.

The Nusselt number of smooth surface is shown for comparison with the rib-roughened surfaces. The rib-roughened surface with p/k=10, 20, 30 augments heat transfer about 2-2.7, 1.8-2.5, 1.7-1.3 times higher than the smooth surface within the Reynolds number range of 4,000 to 40,000. It shows very good heat transfer performance compared to smooth surface. The results show that the two figures are almost same and there is almost no effect on channel heights from the view point of heat transfer augmentation. The case of p/k=10 provides the highest heat transfer augmentation compared to other larger p/k cases; but a degree of heat transfer augmentation is comparatively small.

Figures 36 and 37 show the relationship between the Nusselt number and the Reynolds number for water-flow channel with 1 and 3 mm of height, which was calculated with the empirical correlations obtained by air-flow experiments. Then, water properties are used instead of air properties into the correlations to verify the air correlations whether could be used or not to the water-flow experiments. The rib-roughened surface augments heat transfer about 2-3.2, 1.8-2.9,and 1.6-2.8 times higher than the smooth surface within the range of Reynolds number 2,000 to 1,00,000. Channel heights do not play any important role from the view point of heat transfer augmentation.

2.3 Applicability of correlations obtained by air-flow experiments to water-flow condition

In this section, Webb et al.'s and Liou et al.'s correlations have been verified whether air correlations can be used or not to the water-flow conditions. Webb et al. correlated friction factor and heat transfer data obtained by water-flow experiments and Liou et al. correlated friction factor and heat transfer data obtained by air-flow experiments.

Figure 38 shows the relationship between the friction factor and the Reynolds number in H=1 mm channel as a function of p/k. This figure basically shows the comparison of Webb et al.'s correlations with Liou et al.'s correlations under water-flow conditions. The results show that the difference between the two

correlations are not good agreement; sepecially for p/k=10. The friction factors calculated with the Webb et al.'s correlation are independent of the Reynolds number over the Reynolds number range investigated for both the conditions.

Figures 39 and 40 show the relationship between the Nusselt number and the Reynolds number comparing to Webb et al.'s correlations with Liou et al.'s correlations under water-flow and air-flow conditions in H=1 mm channel. The results show that there is a large difference between Webb et al.'s and Liou et al.'s correlations under water and air flow conditions.

Figures 41, 42 and 43 show the same figures as Figs. 38, 39 and 40 whose channel height is H=3 mm. From these figures, the results also show that the difference between the two correlations are little bit small compared to channel height of H=1 mm, but some curves calculated by Liou et al.'s correlations cross over the another curves calculated by Webb et al.'s correlations. The causes for this difference would be that the surface roughness have a larger effect on heat transfer at high Prandtl numbers where the heat transfer resistance is more concentrated in the sublayers than at low Prandtl numbers for air. From another point of view, the reason seems to be that since repeated-rib surface may be viewed as a problem in boundary layer separation and reattachment, 0.2 mm rib-height will break the sublayer where molecular effects dominant by creating turbulence which means high heat transfer augmentation for water flows. But for gas flows, 0.2 mm rib-height should be over the buffer layer region where molecular effects still significant but not dominant to augment heat transfer by creating turbulence.

The inspection of these curves reveals the similar tendency. So, from these figures 38, 39, 40, 41, 42 and 43, the important finding made by them is that for fully developed turbulent flow in channels, correlations obtained by air-flow experiments have showed lower heat transfer performance than the water-flow conditions.

Table 1-1 Experimental condition

Webb et al.					
Experimental Apparatus	Tube	Rib height k,	Rib pitch p, mm	Rib width w, mm	Tube diameter D,mm
	01/10	0.37	3.7	0.38	36.8
	02/10	0.74	7.3	0.38	36.8
	04/10	1.5	14.7	0.38	36.8
	02/20	0.74	14.7	0.38	36.8
	02/40	0.74	29.4	0.38	36.8
Pressure	0.17MPa				
Temperature	34℃				
Flow velocity	0.14-2.3 m/s				
Reynolds number	6000-10^5				

Table 1-2 Experimental condition

Liou et al.				
Experimental Apparatus	Rib type	Rib height k, mm	Rib pitch p, mm	Channel height H, mm
	Square	5.2	52,78,104	40
	Triangular	5.2	52,78,104	40
	Semi circular	5.2	52,78,104	40
Pressure	0.1MPa			
Temperature	25℃			
Flow velocity	1.9 -12.5 m/s			
Reynolds number	7800-50000			

Table 2 Constants in correlations [14] and [17]

Square ribs	a_1	a_2	a_3
	11.752	-0.137	-0.121
	b_1	b_2	b_3
	0.684	-0.109	-0.606

Table 3 Proposed experimental condition

Fluid	: Water
Reynolds number	: 6000 ~ 100000
Flow velocity	< 30 m/s
Inlet temperature	< 15 °C
Heat flux	< 1MW/m^2
System pressure	< 1.5 MPa
Flow direction	: Vertical
Flow condition	: Fully developed turbulent flow
Heating condition	: Uniform heating from one side

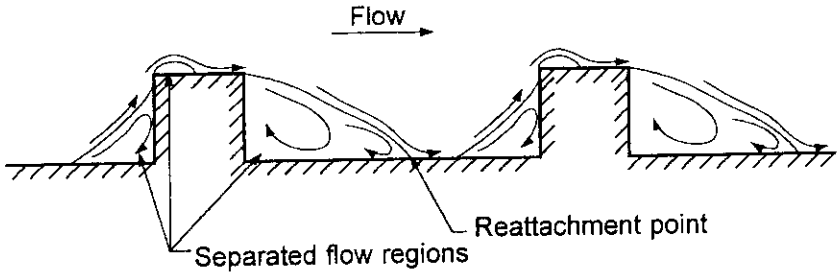

Fig.1 Schematic representation of flow pattern on rib-roughened surface

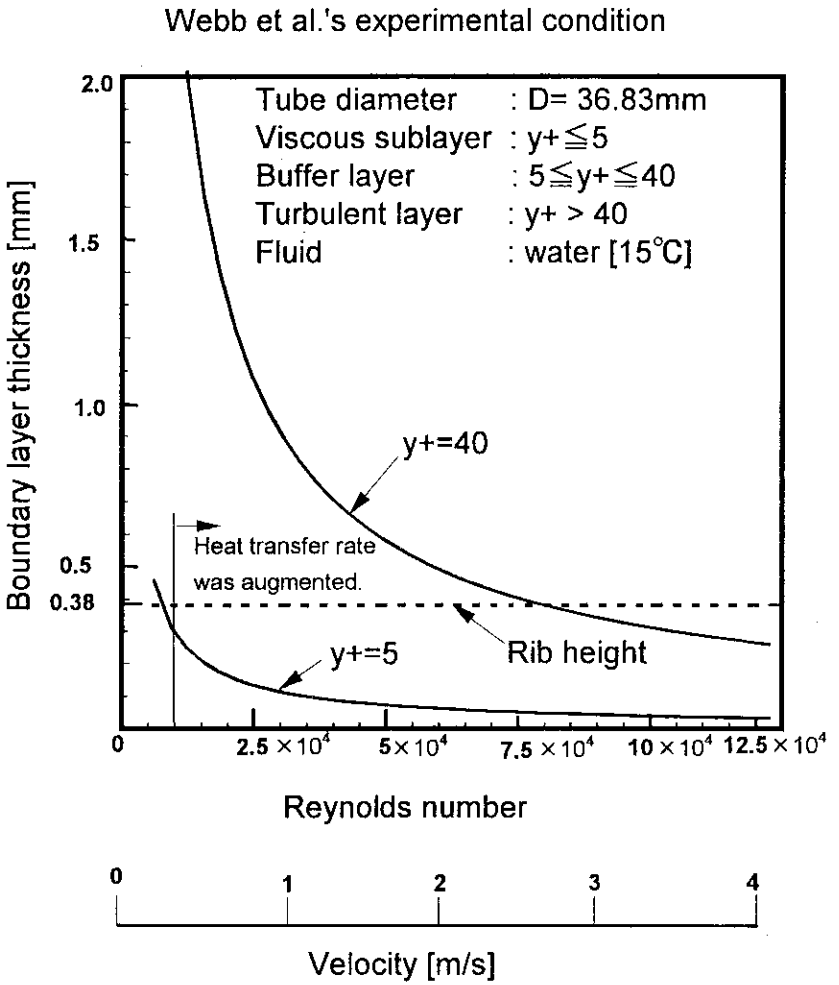

Fig. 2 Relationship between Reynolds number and boundary layer thickness

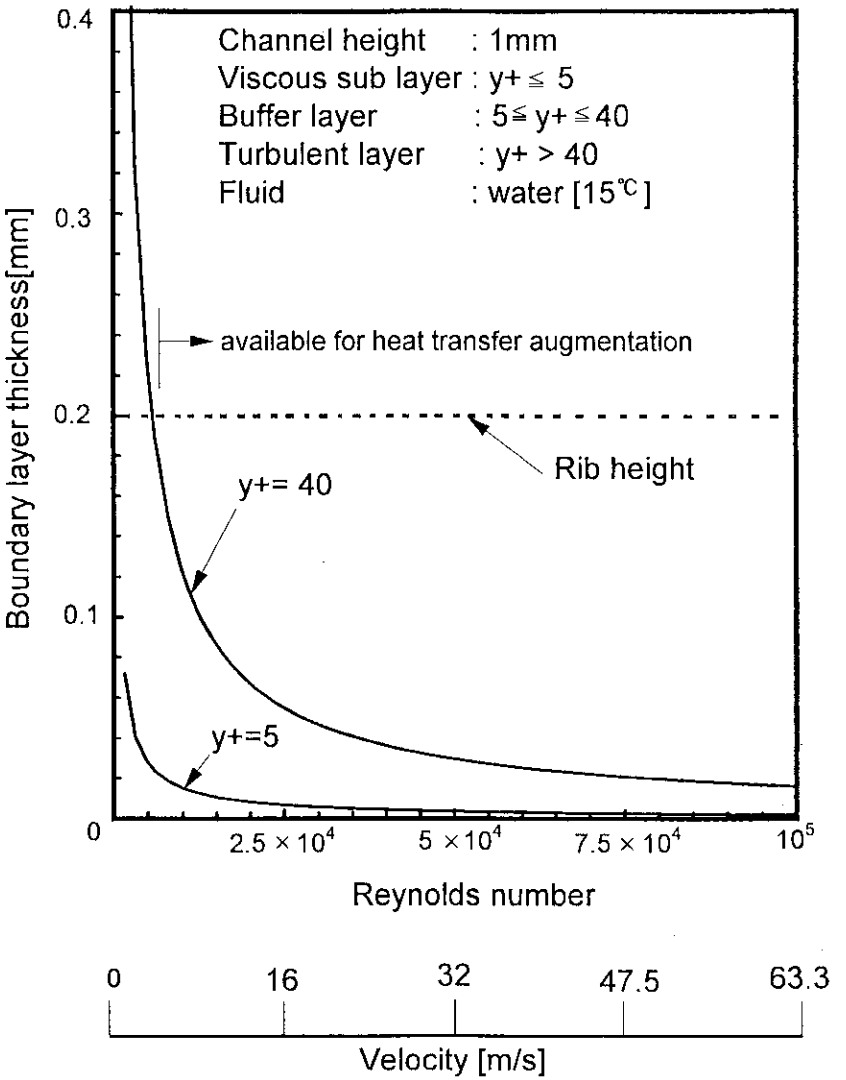

Fig.3 Relationship between Reynolds number and boundary layer thickness

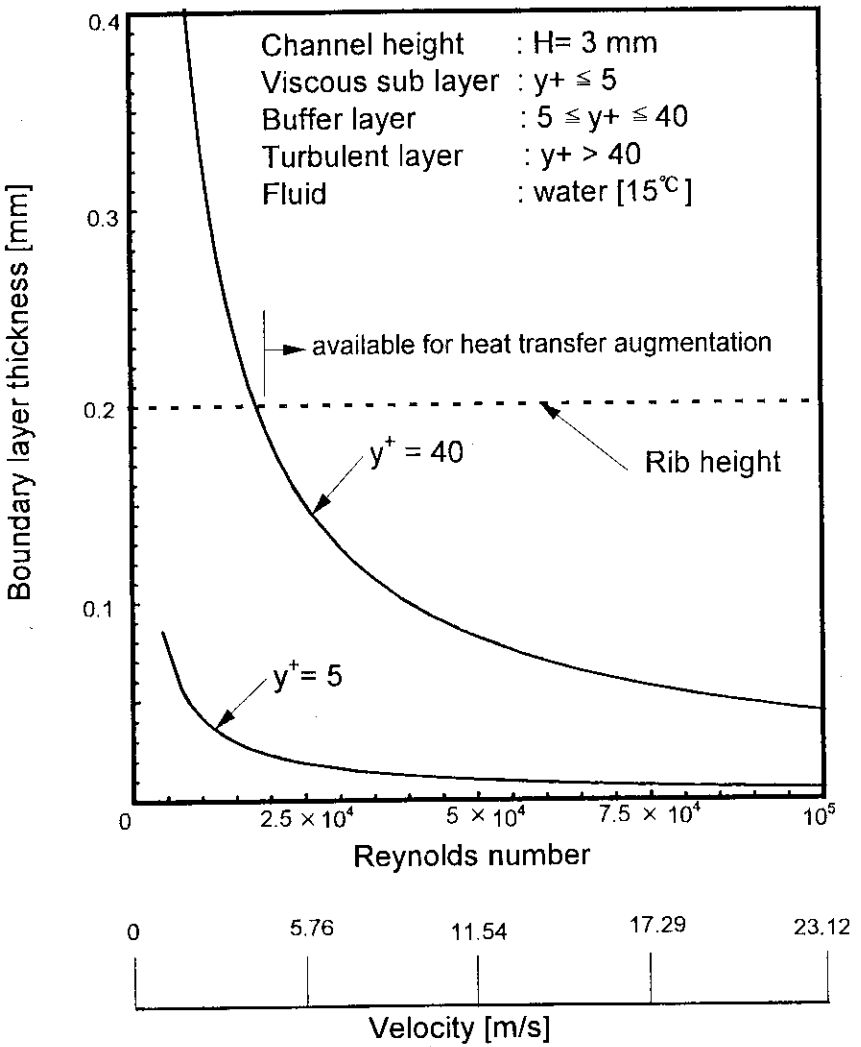

Fig.4 Relationship between Reynolds number and boundary layer thickness

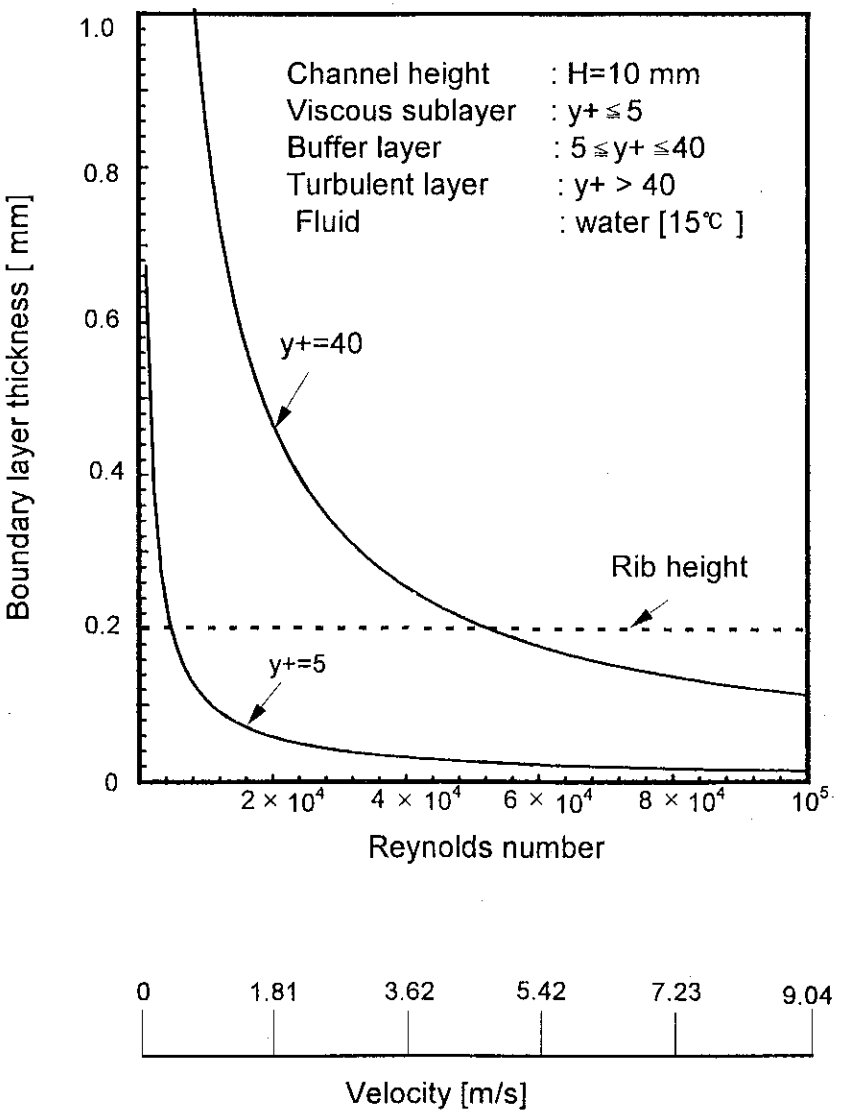

Fig.5 Relationship between Reynolds number and boundary layer thickness

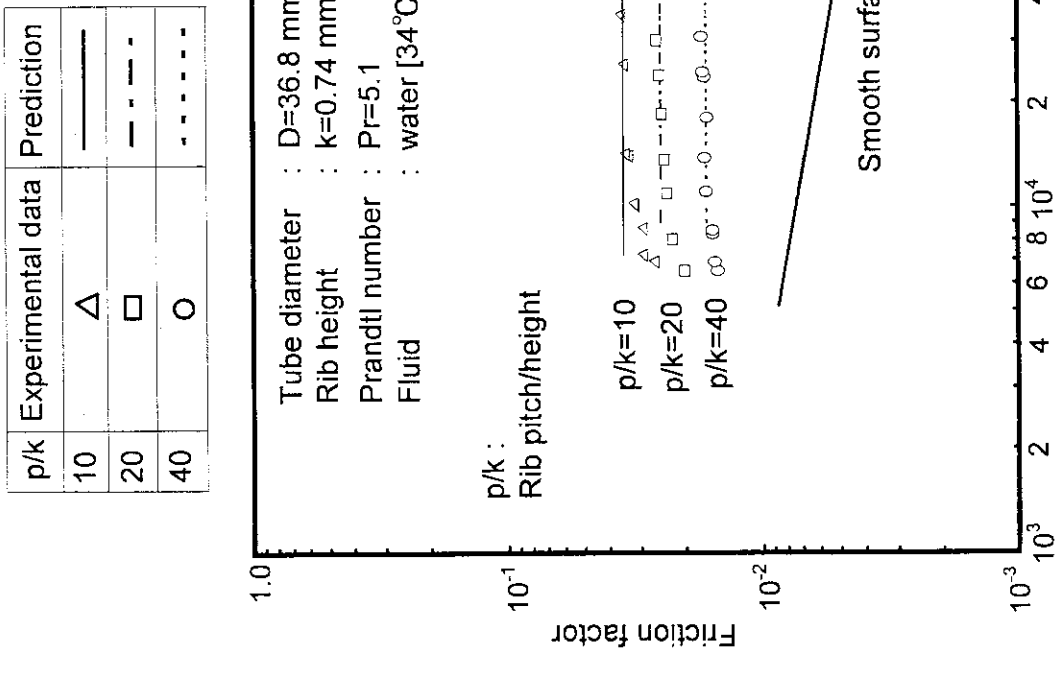

p/k	Experimental data	Prediction
10	△	———
20	□	— - — -
40	○	- - - - - -

Fig. 6 Comparison of friction factor predictions with the data of Webb et al. for the k/D=0.02, w/k=0.52 and varying p/k ratios.

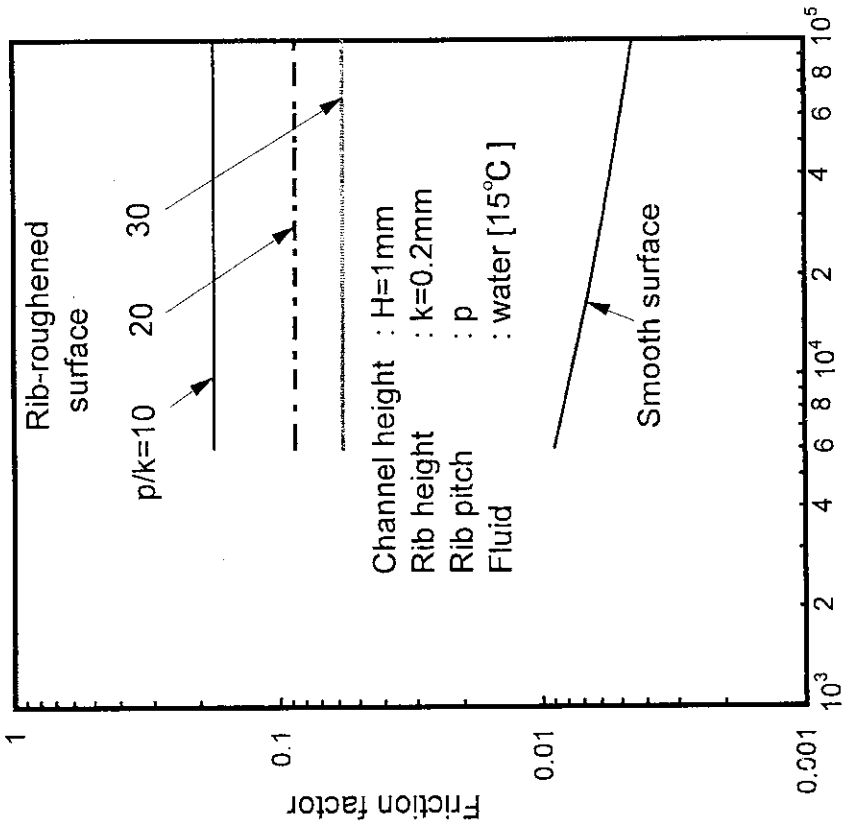

Fig. 7 Relationship between friction factor and Reynolds number [Webb et al.]

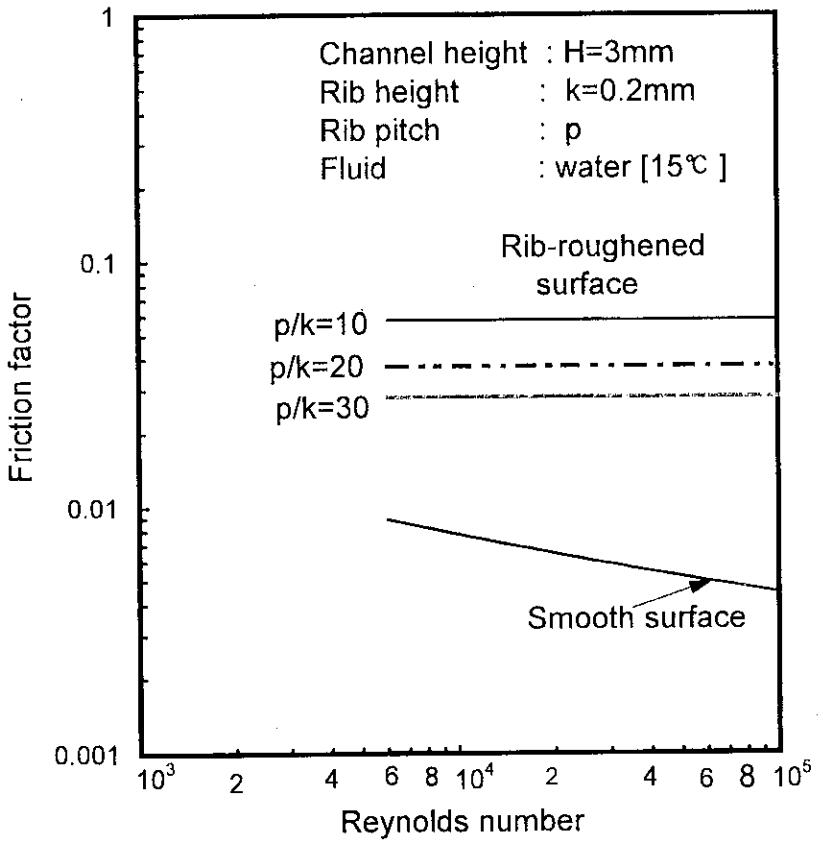

Fig. 8 Relationship between friction factor and Reynolds number [Webb et al.]

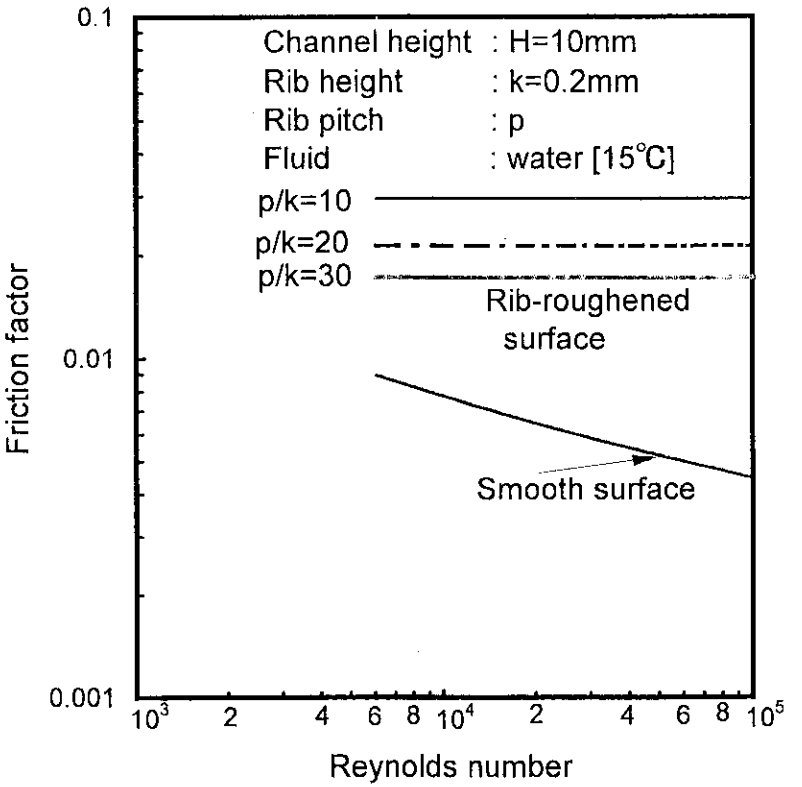

Fig.9 Relationship between friction factor and Reynolds number [Webb et al.]

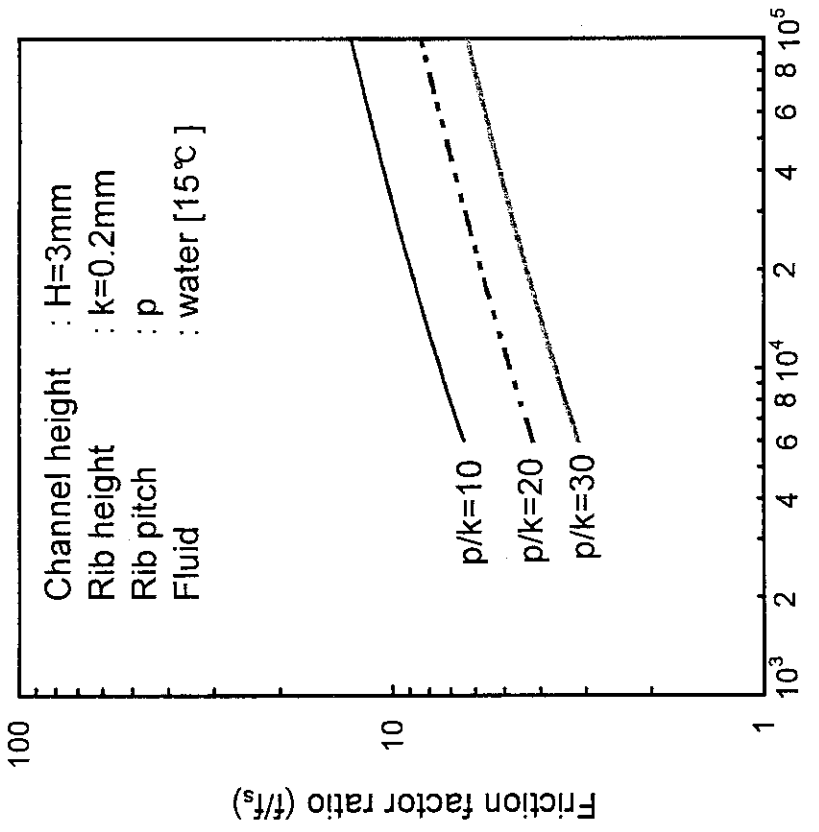

Fig.11 Relationship between friction factor ratio and Reynolds number [Webb et al.]

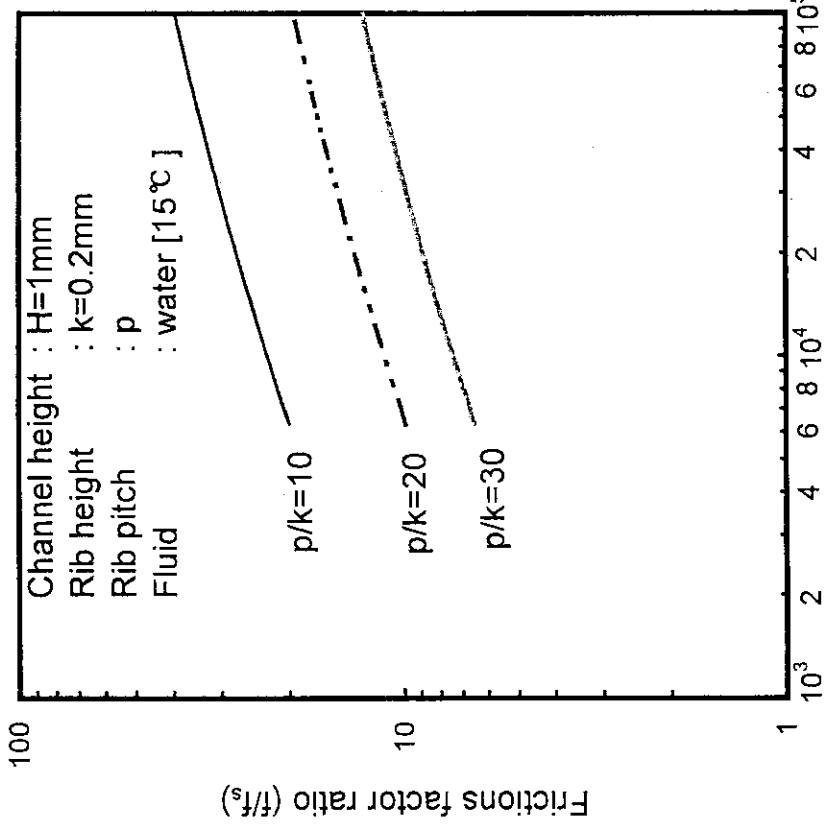

Fig.10 Relationship between friction factor ratio and Reynolds number [Webb et al.]

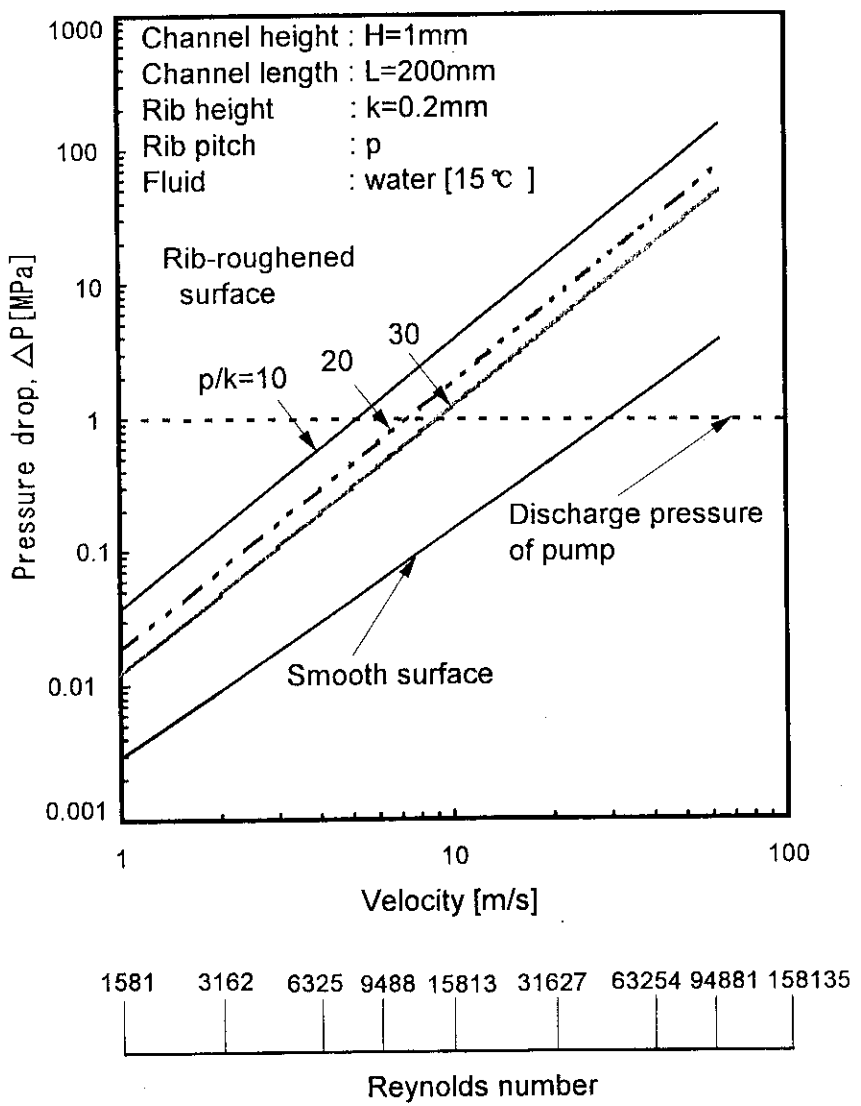

Fig.12 Relationship between pressure drop and water velocity [Webb et al.]

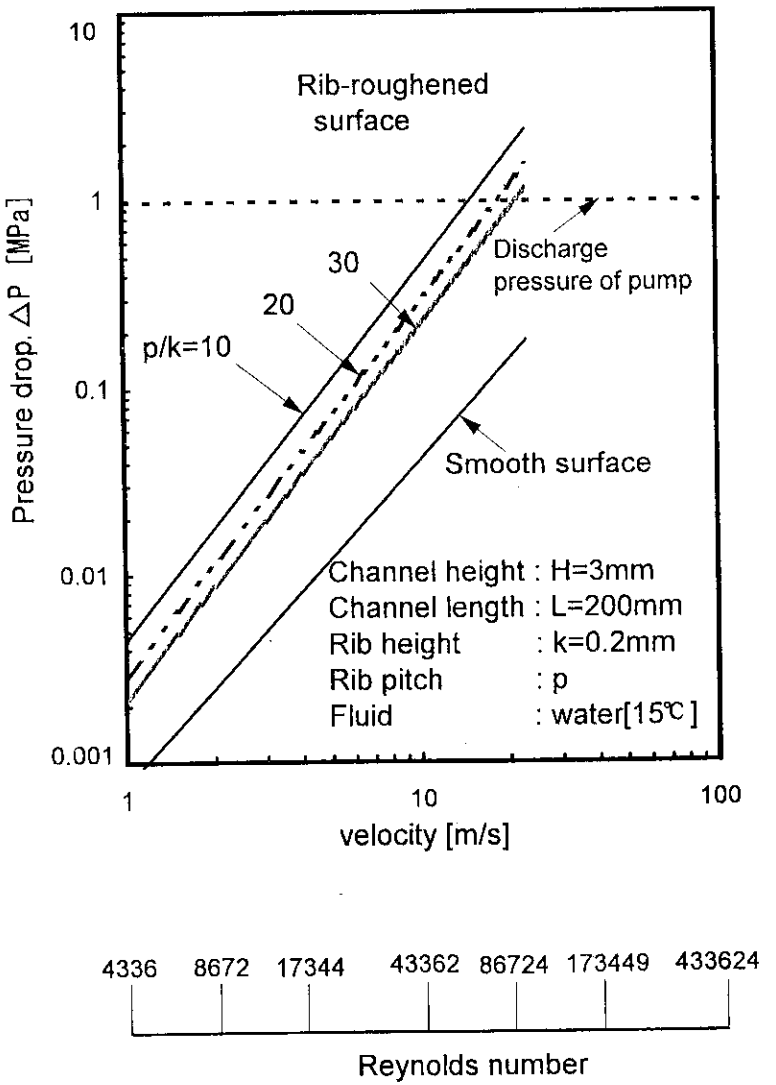

Fig.13 Relationship between pressure drop and water velocity [Webb et al.]

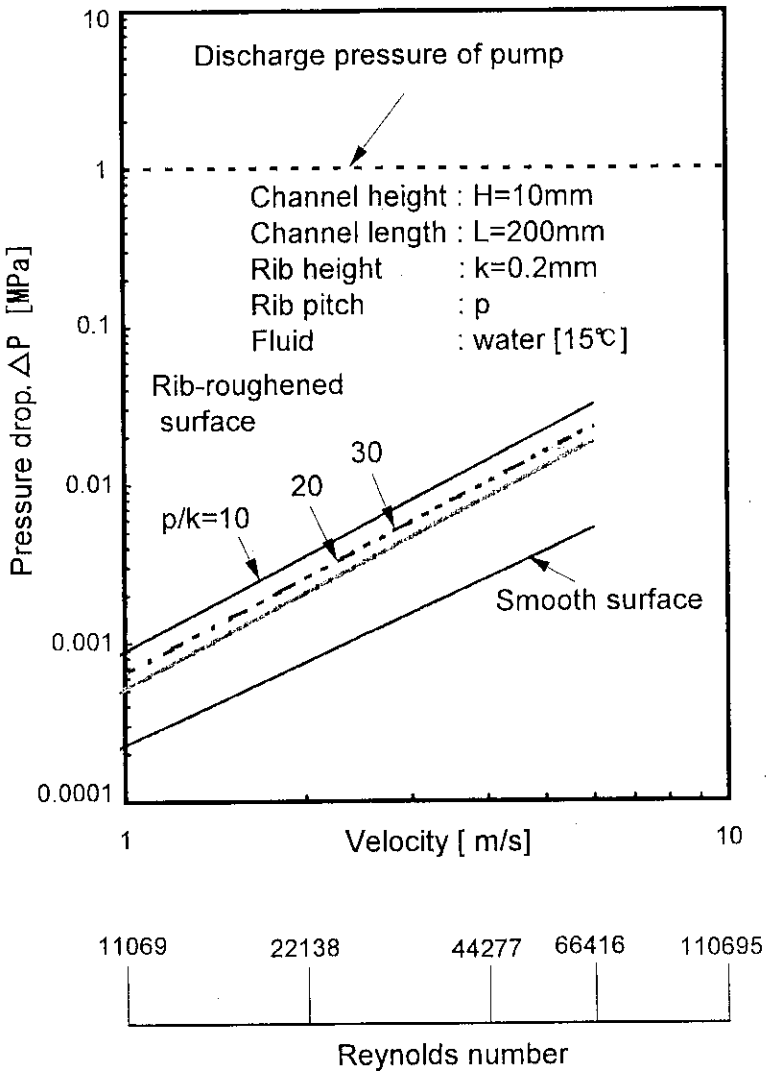

Fig.14 Relationship between pressure drop and water velocity [Webb et al.]

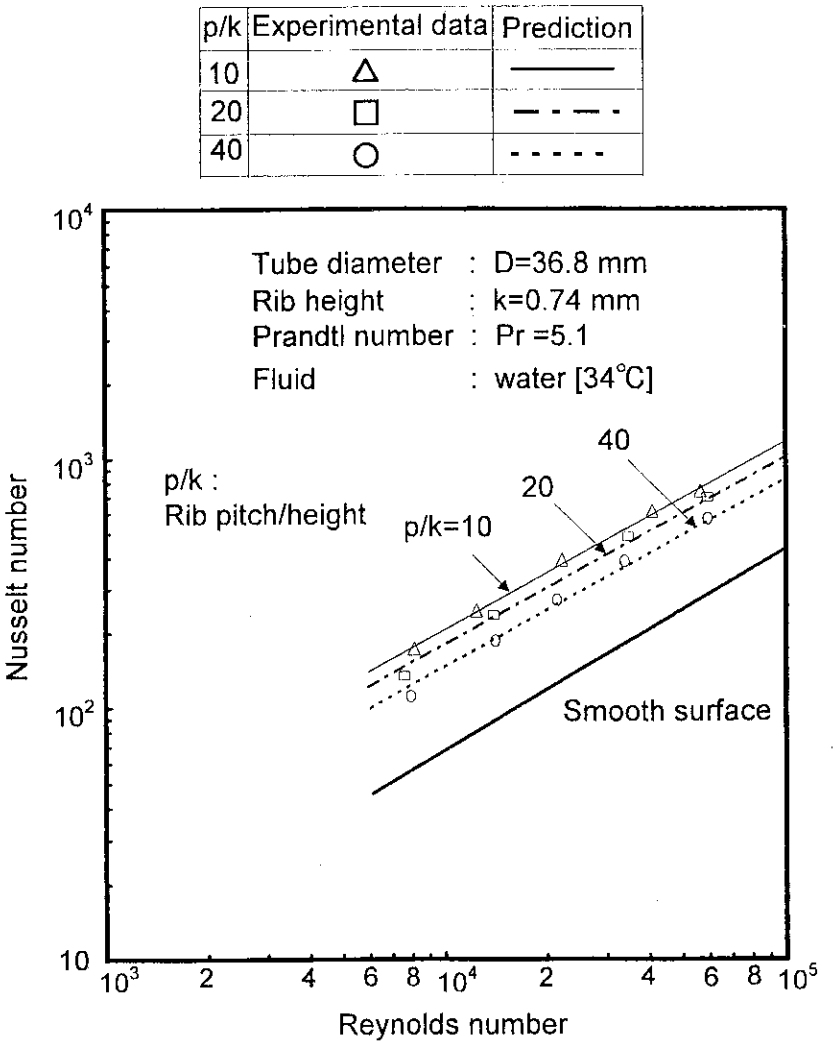

Fig.15 Comparison of Nusselt number predictions with the data of Webb et al. for the k/D=0.02, w/k=0.52 and varying p/k ratios.

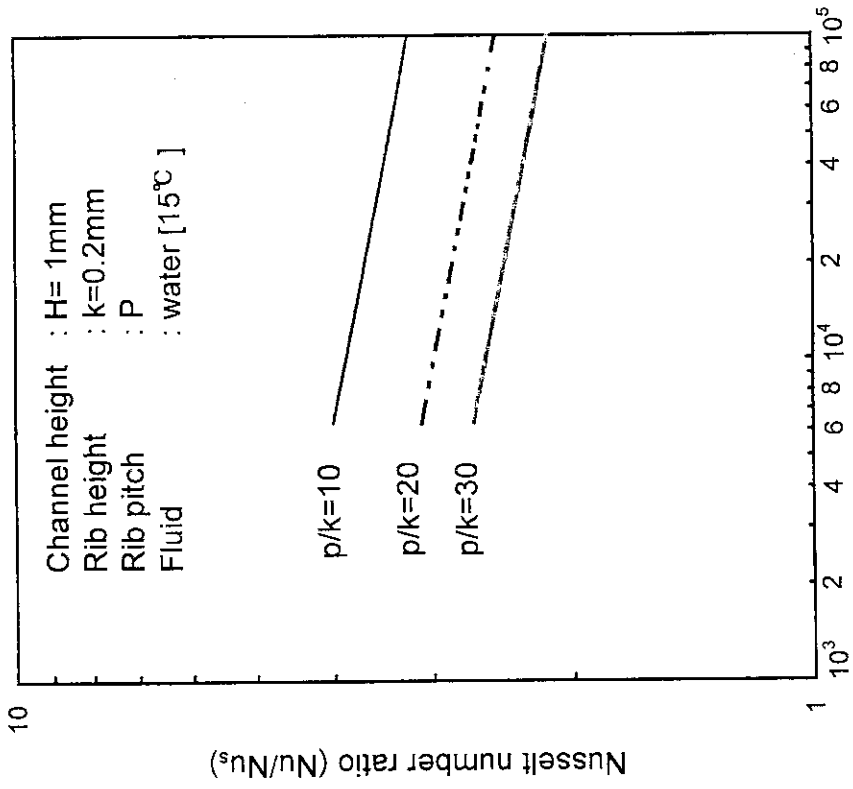

Fig.17 Relationship between Nusselt number ratio and Reynolds number [Webb et al.]

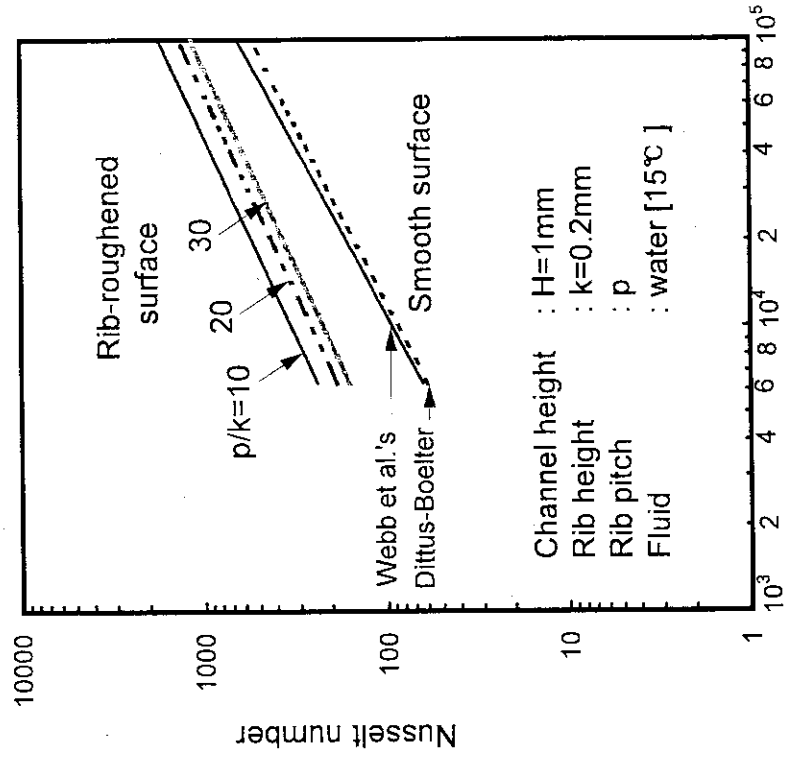

Fig.16 Relationship between Nusselt number and Reynolds number [Webb et al.]

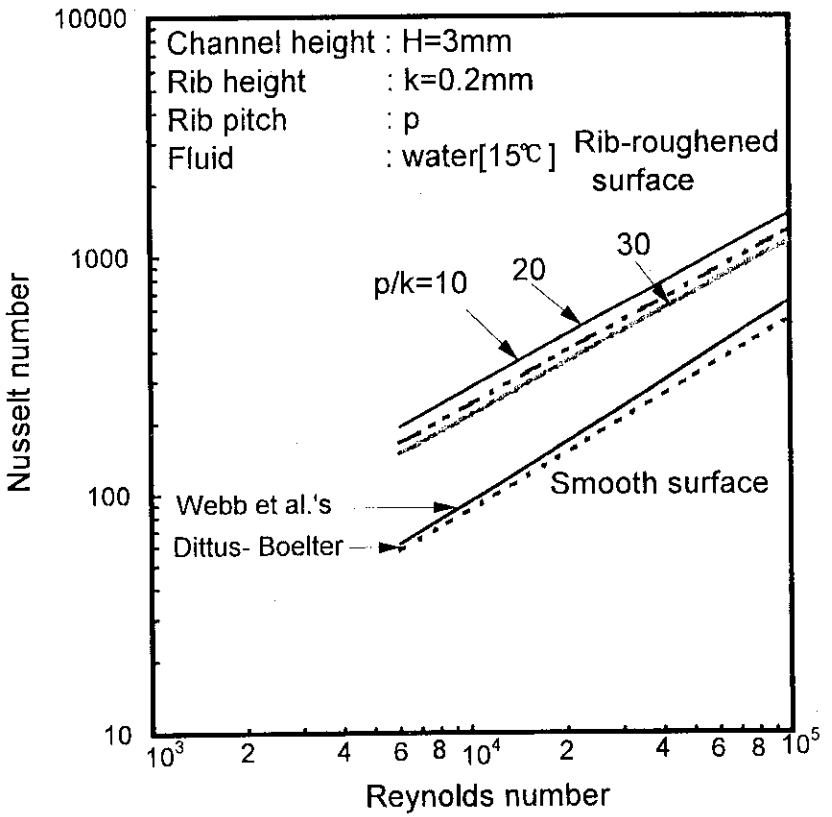

Fig.18 Relationship between Nusselt number and Reynolds number [Webb et al.]

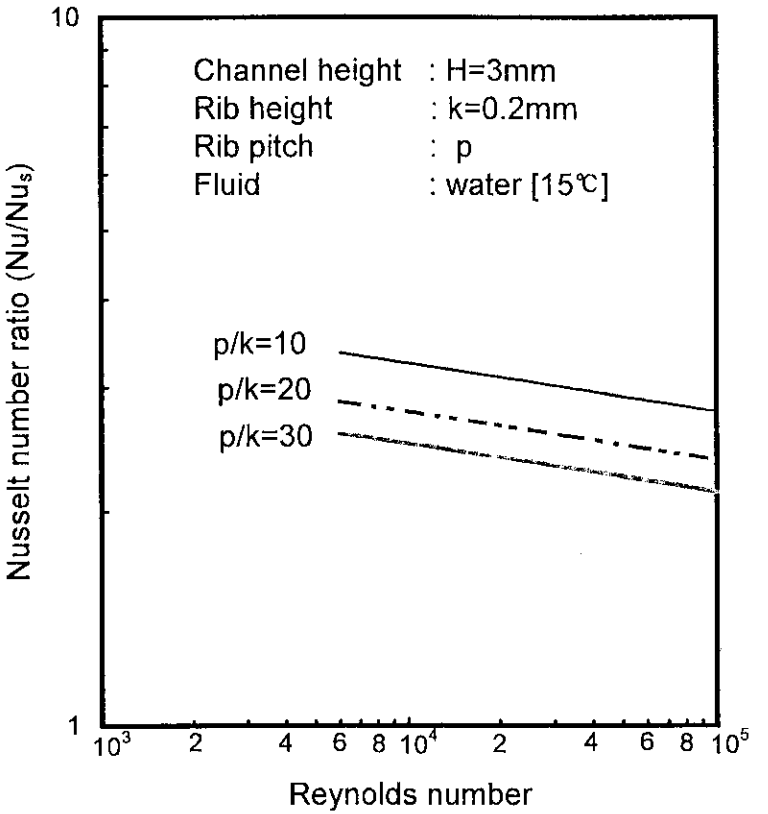

Fig.19 Relationship between Nusselt number ratio and Reynolds number [Webb et al.]

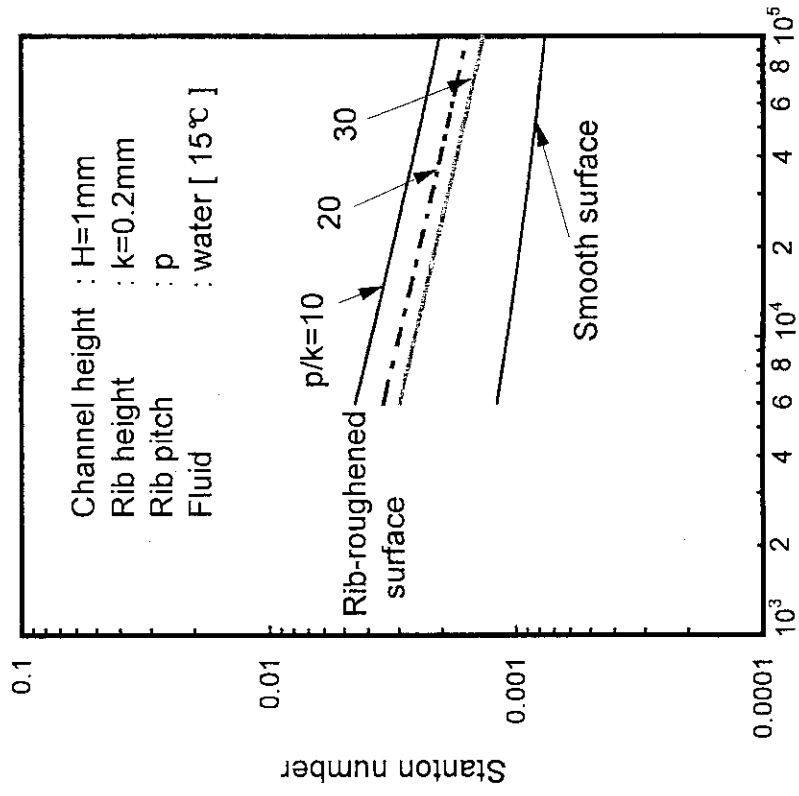

Fig.21 Relationship between Stanton number and Reynolds number [Webb et al.]

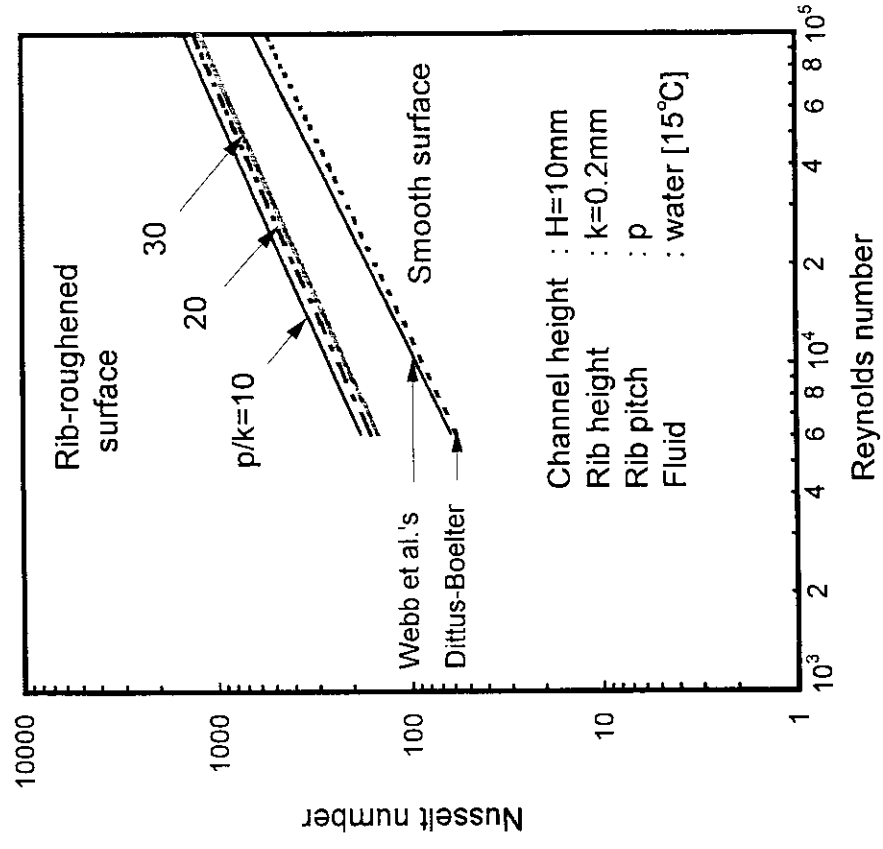

Fig .20 Relationship between Nusselt number and Reynolds number [Webb et al.]

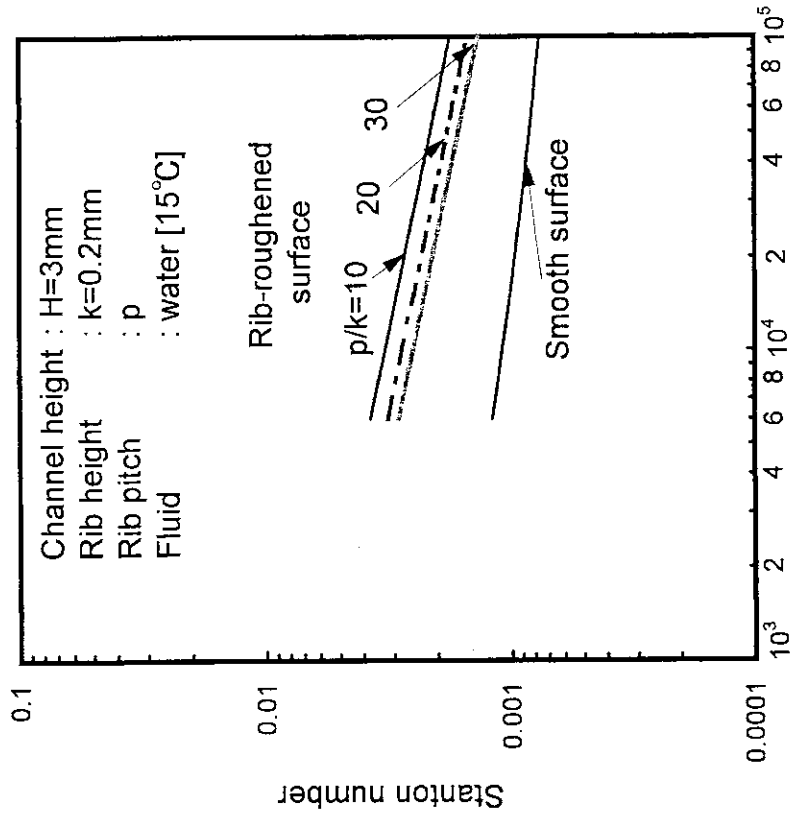

Fig.23 Relationship between Stanton number and Reynolds number [Webb et al.]

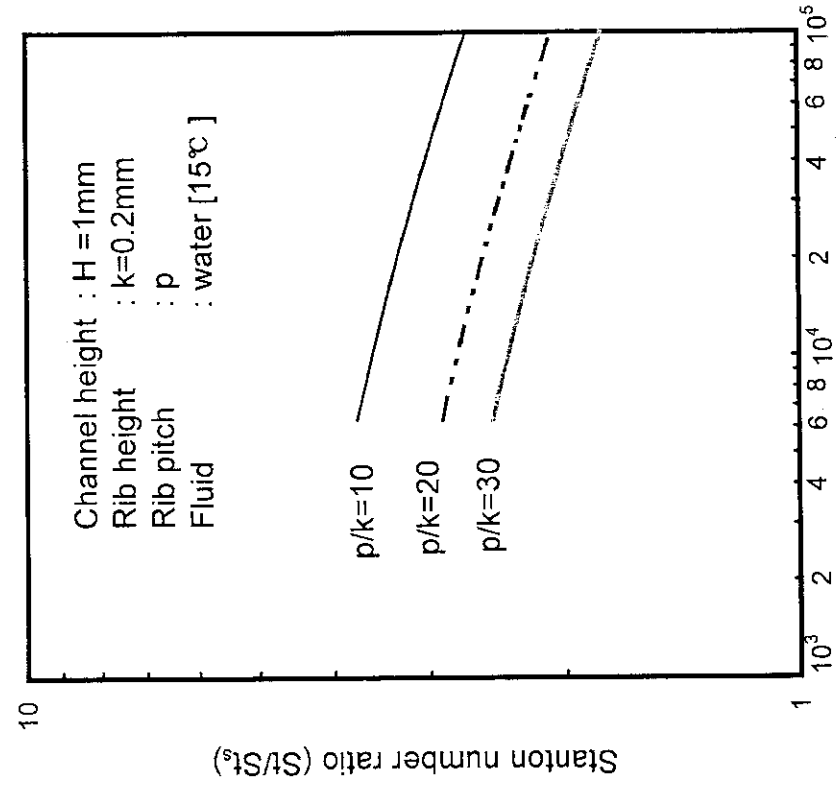

Fig.22 Relationship between Stanton number ratio and Reynolds number [Webb et al.]

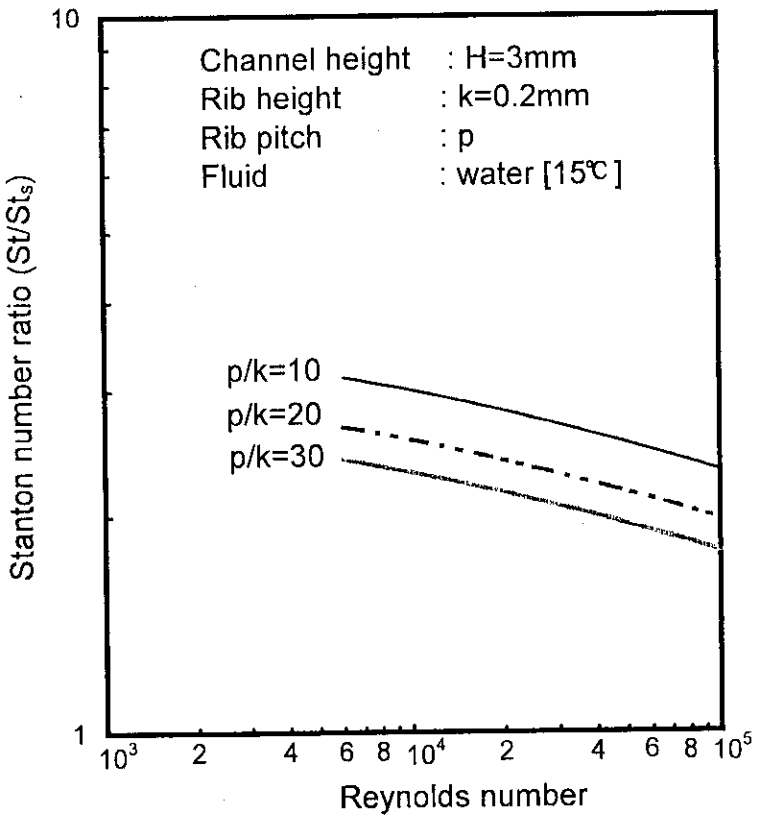

Fig.24 Relationship between Stanton number ratio and Reynolds number [Webb et al.]

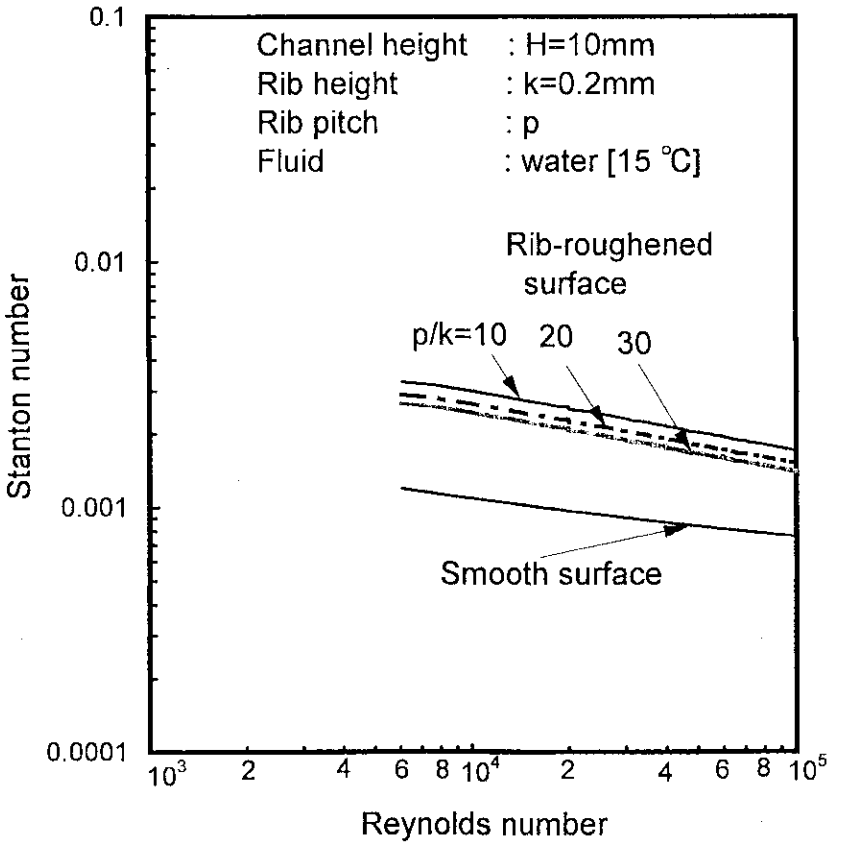

Fig. 25 Relationship between Stanton number and Reynolds number [Webb et al.]

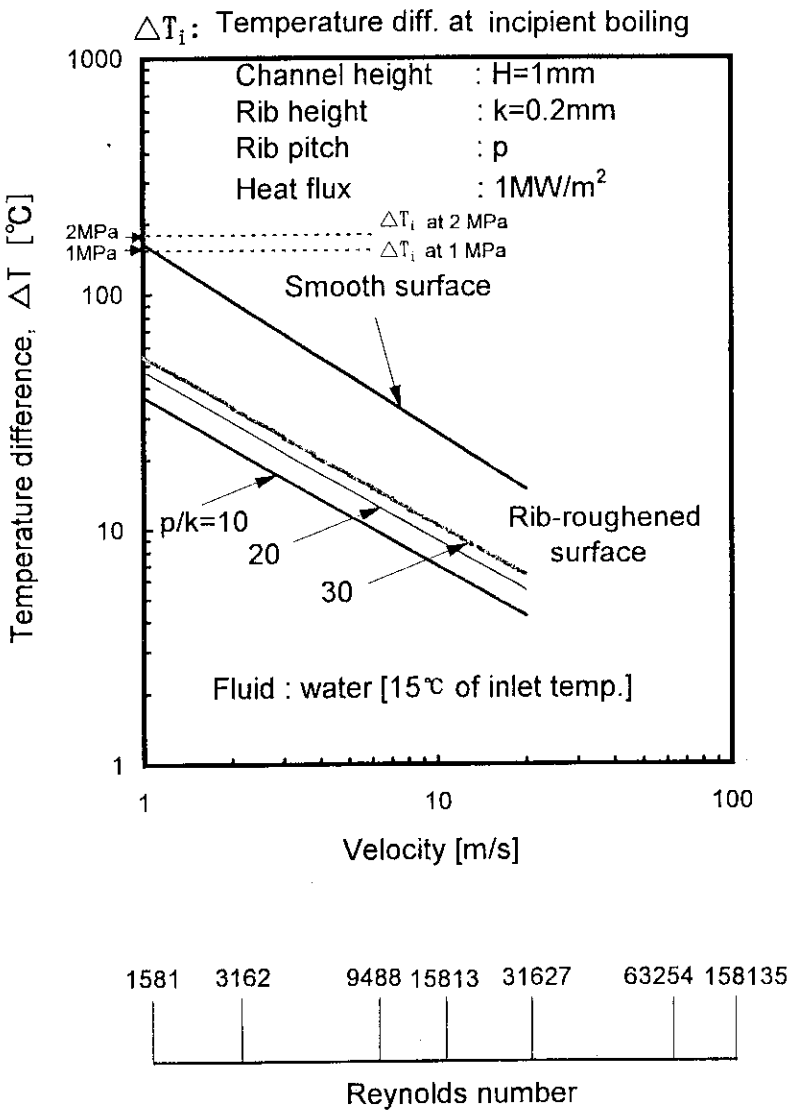

Fig. 26 Relationship between temperature difference and water velocity [Webb et al.]

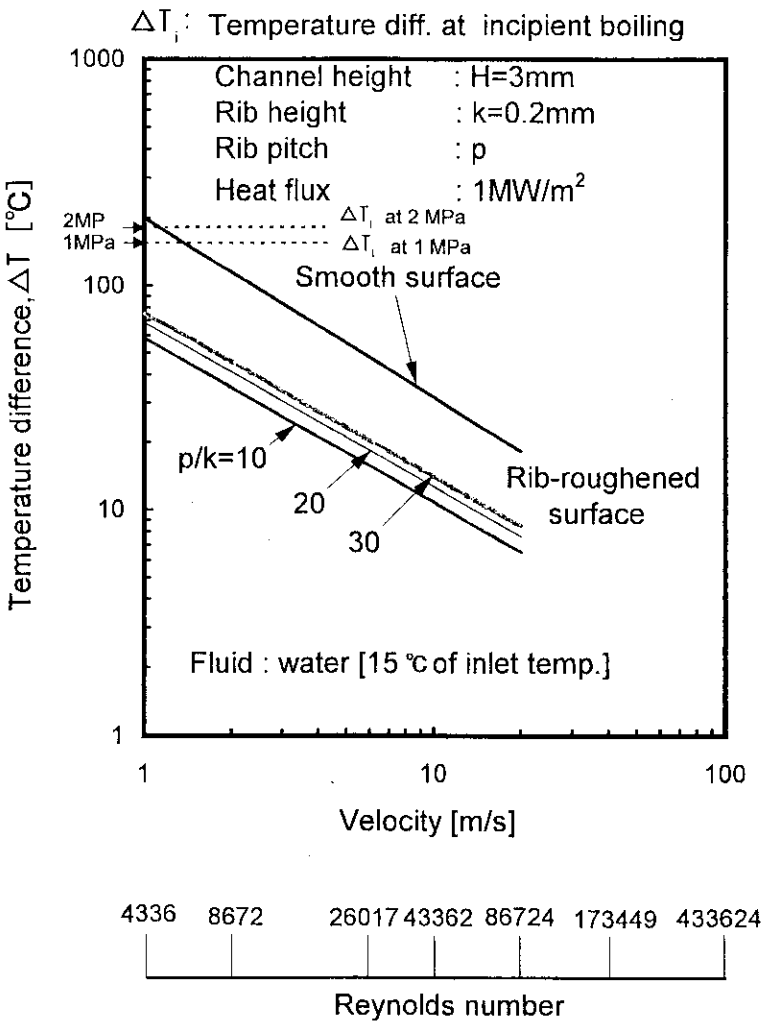

Fig. 27 Relationship between temperature difference and water velocity [Webb et al.]

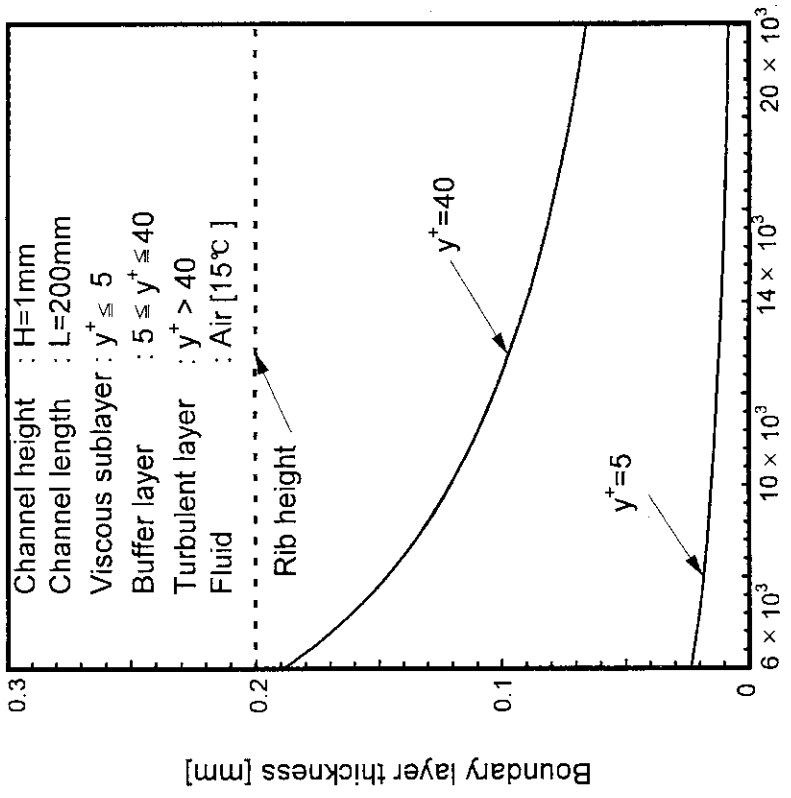

Fig.29 Relationship between Reynolds number and boundary layer thickness

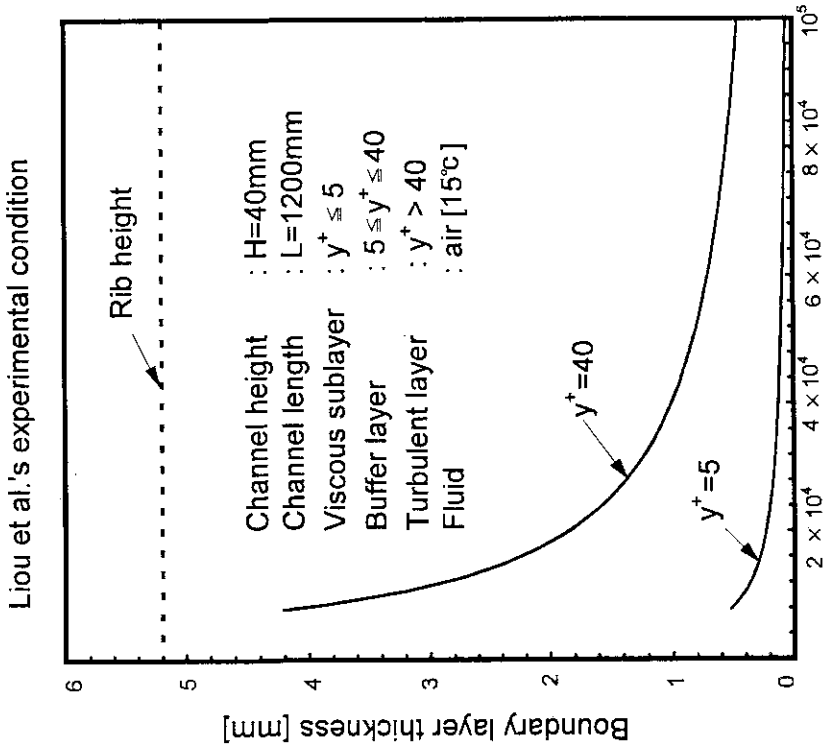

Fig.28 Relationship between Reynolds number and boundary layer thickness

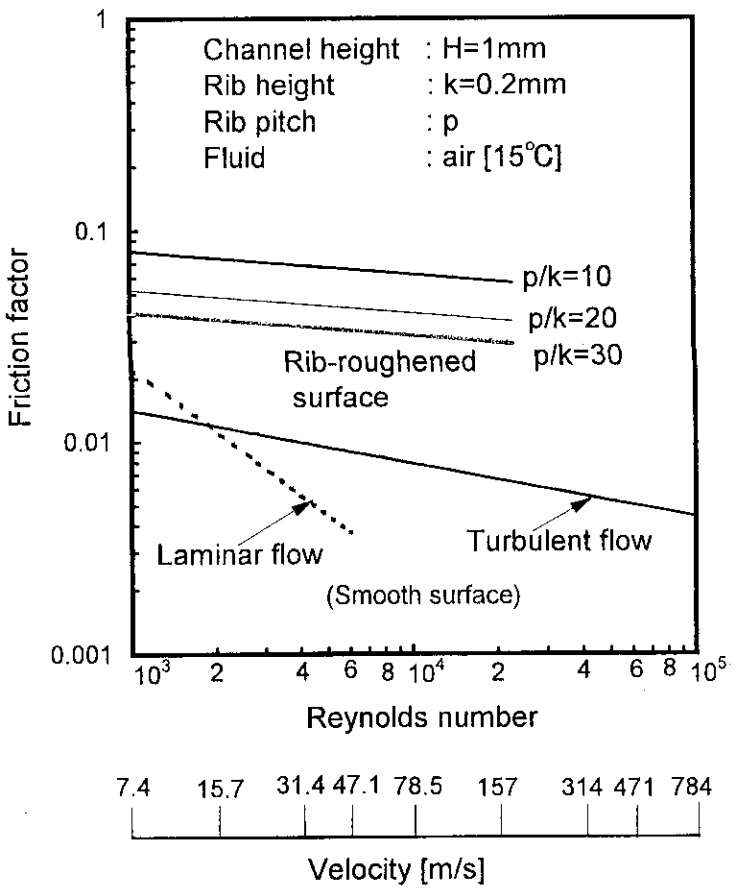

Fig.30 Relationship between friction factor and Reynolds number for air from the emperical correlations obtained by air expt.

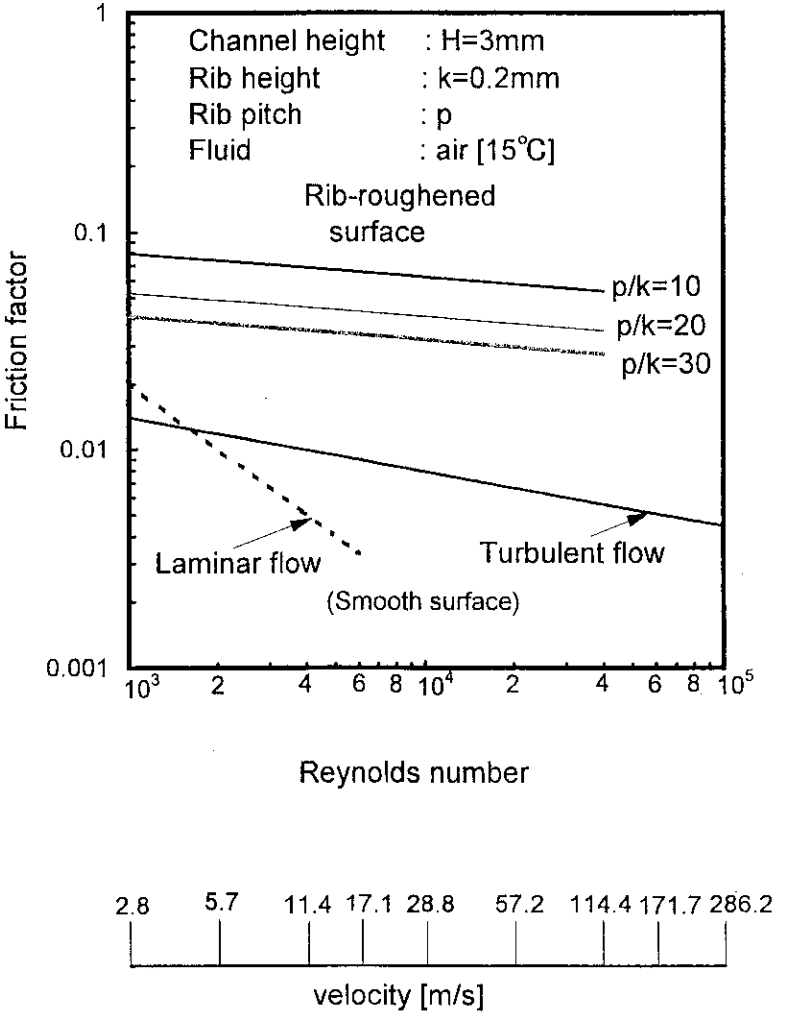

Fig.31 Relationship between friction factor and Reynolds number for air from the emperical correlations obtained by air expt.

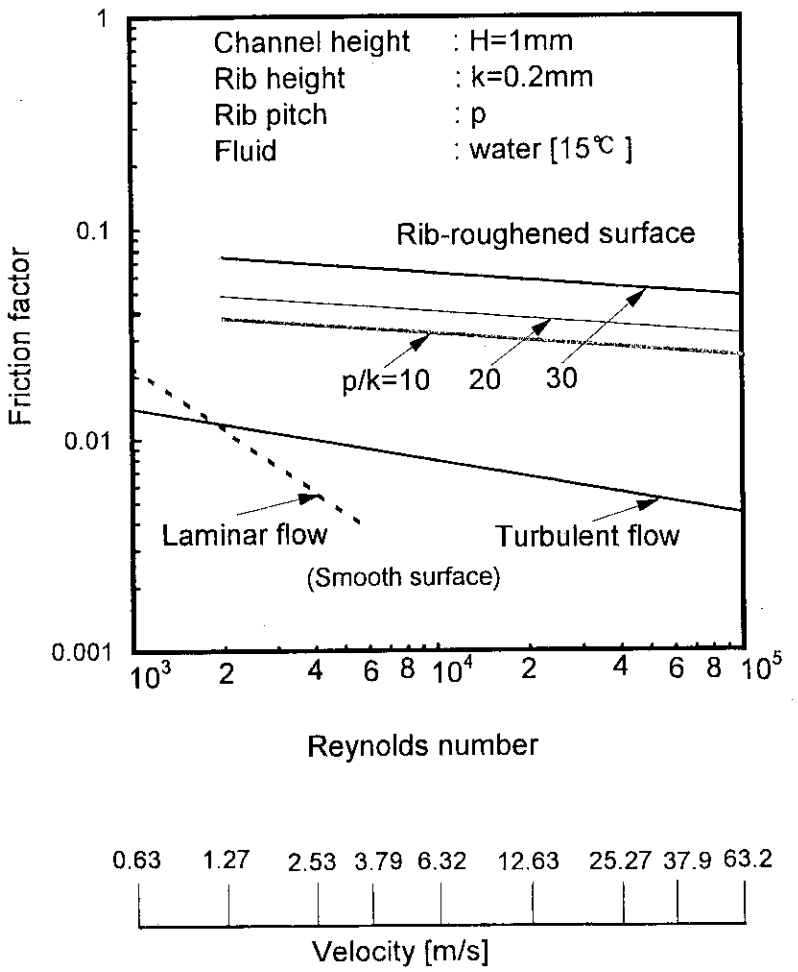

Fig.32 Relationship between friction factor and Reynolds number for water from the emperical correlations obtained by air expt.

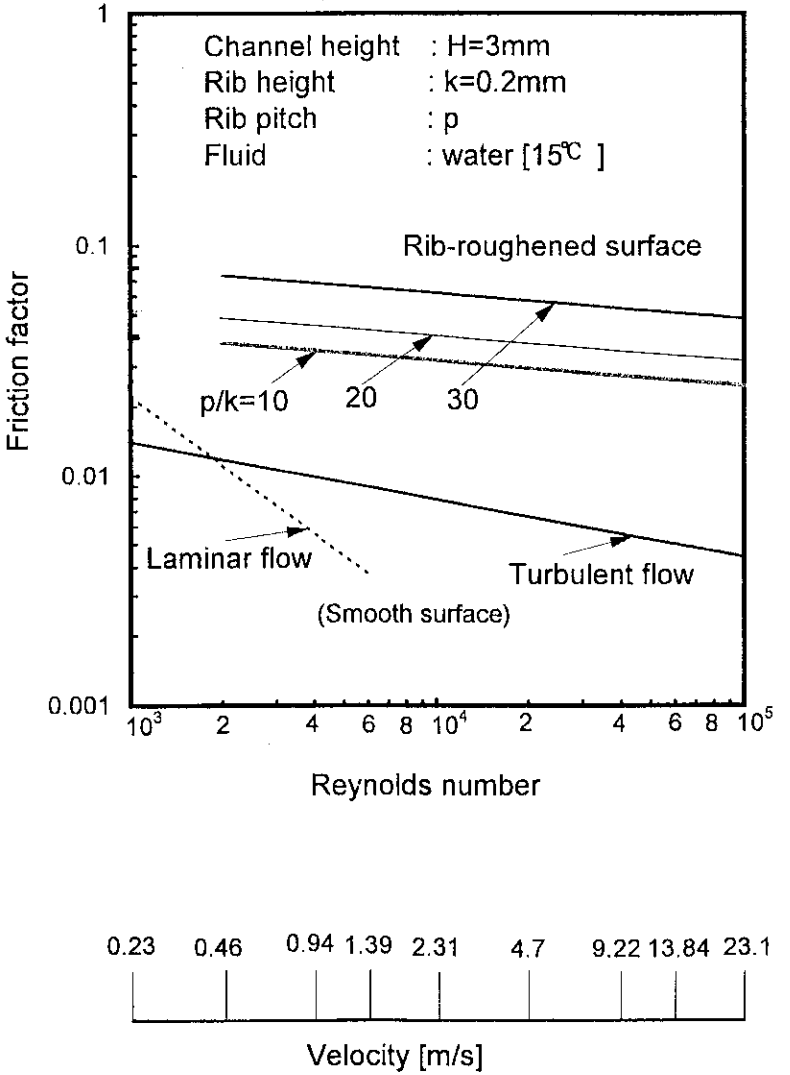

Fig.33 Relationship between friction factor and Reynolds number for water from the emperical correlations obtained by air expt.

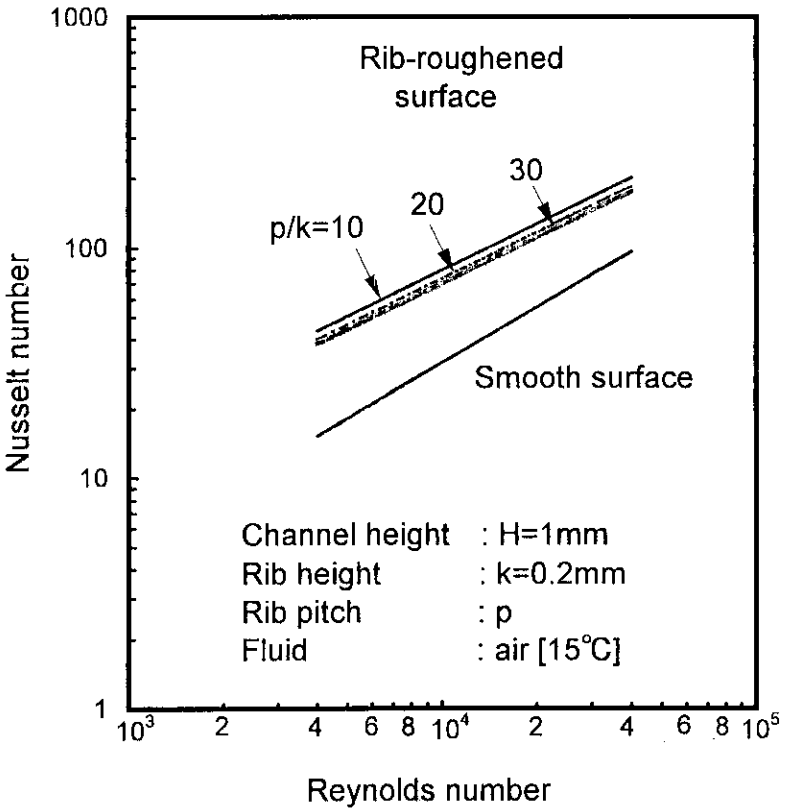

Fig.34 Relationship between Nusselt number and Reynolds number for air from the emperical correlations obtained by air expt.

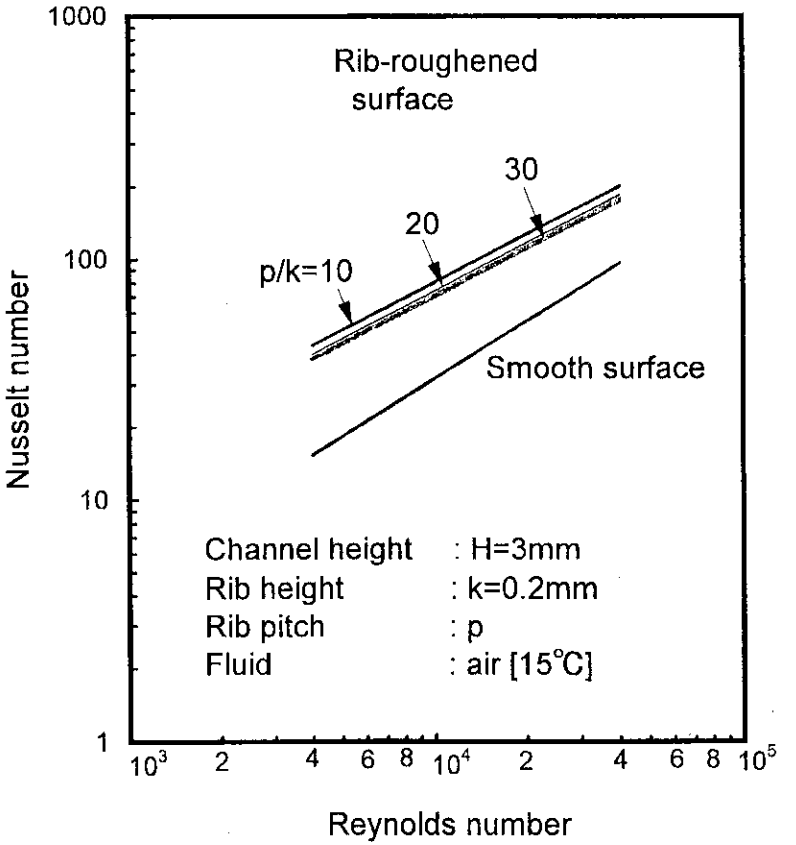

Fig.35 Relationship between Nusselt number and Reynolds number for air from the emperical correlations obtained by air expt.

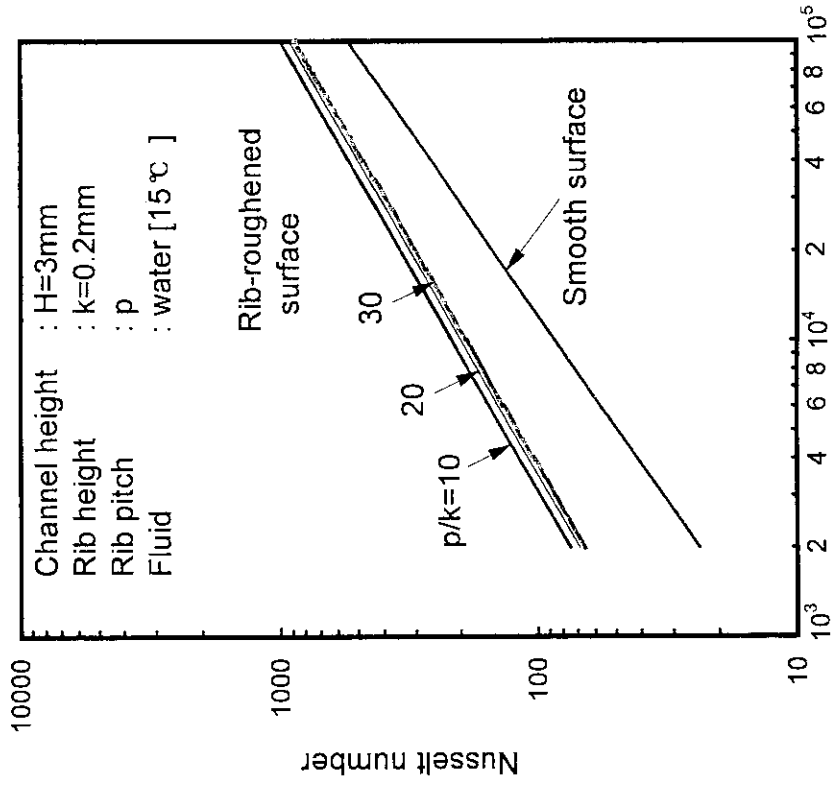

Fig.37 Relationship between Nusselt number and Reynolds number for water from the emperical correlations obtained by air expt.

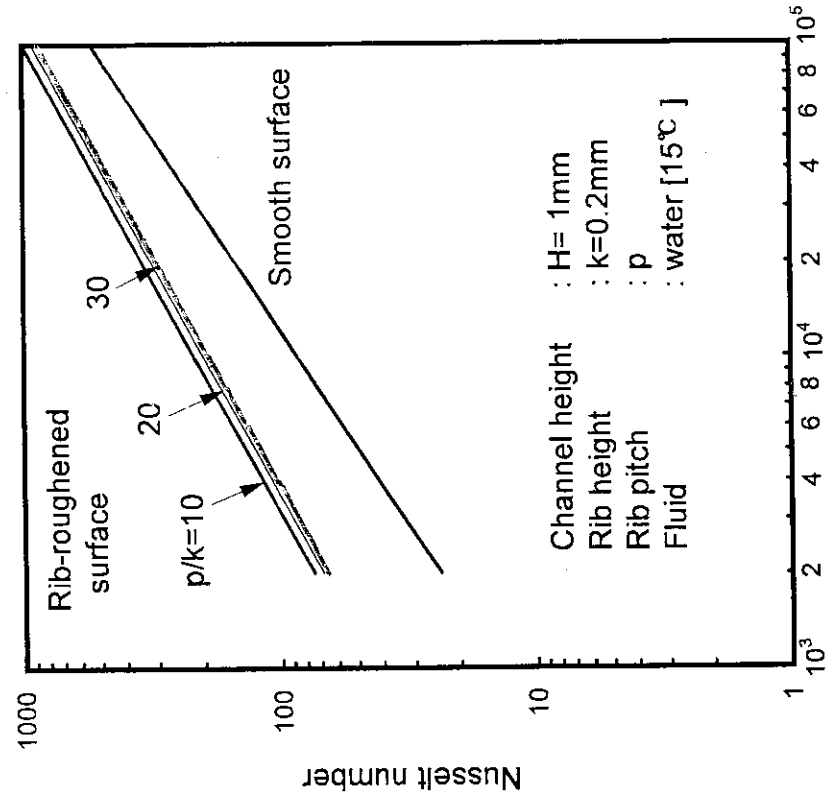

Fig.36 Relationship between Nusselt number and Reynolds number for water from the emperical correlations obtained by air expt.

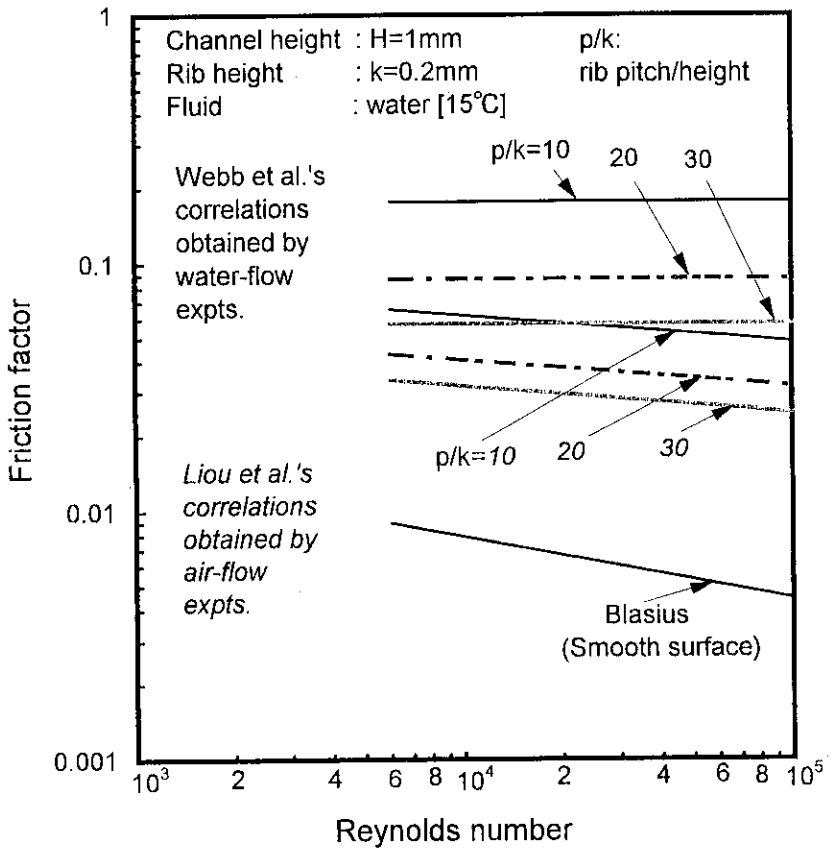

Fig.38 Comparison of Webb et al.'s correlations with Liou et al.'s correlations under water flow condition.

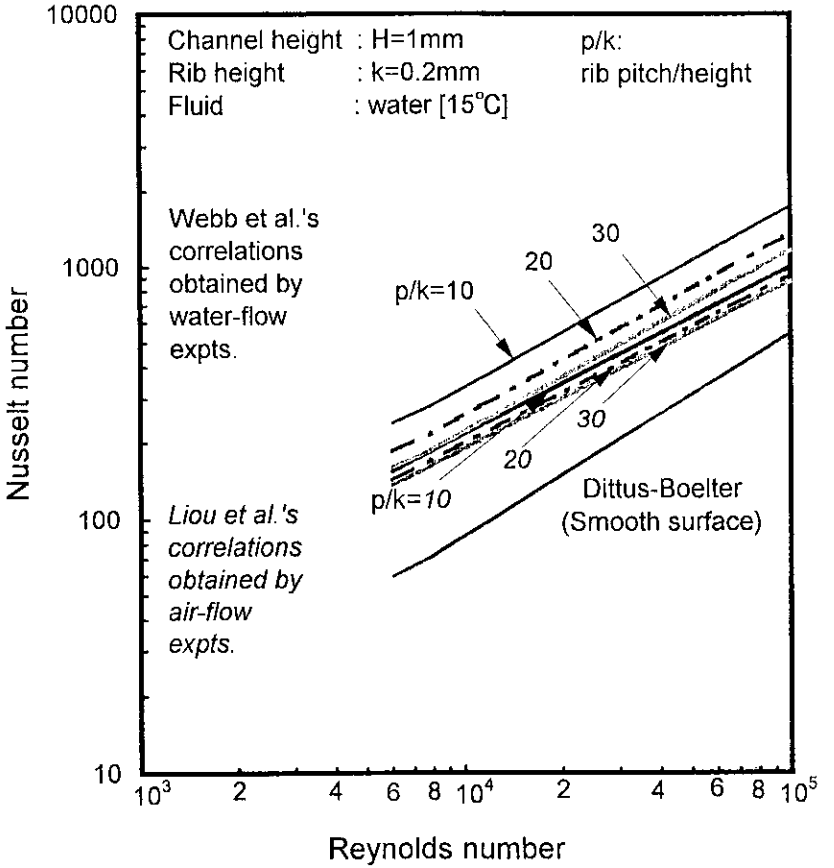

Fig.39 Comparison of Webb et al.'s correlations with Liou et al.'s correlations under water flow condition.

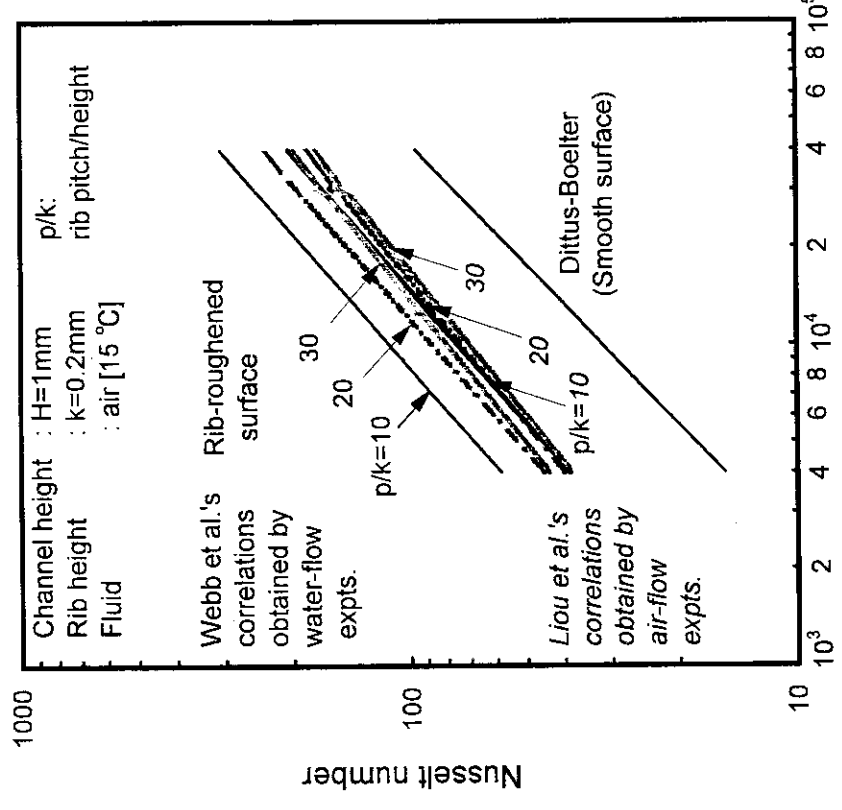

Fig.40 Comparison of Webb et al.'s correlations with Liou et al.'s correlations under air flow condition.

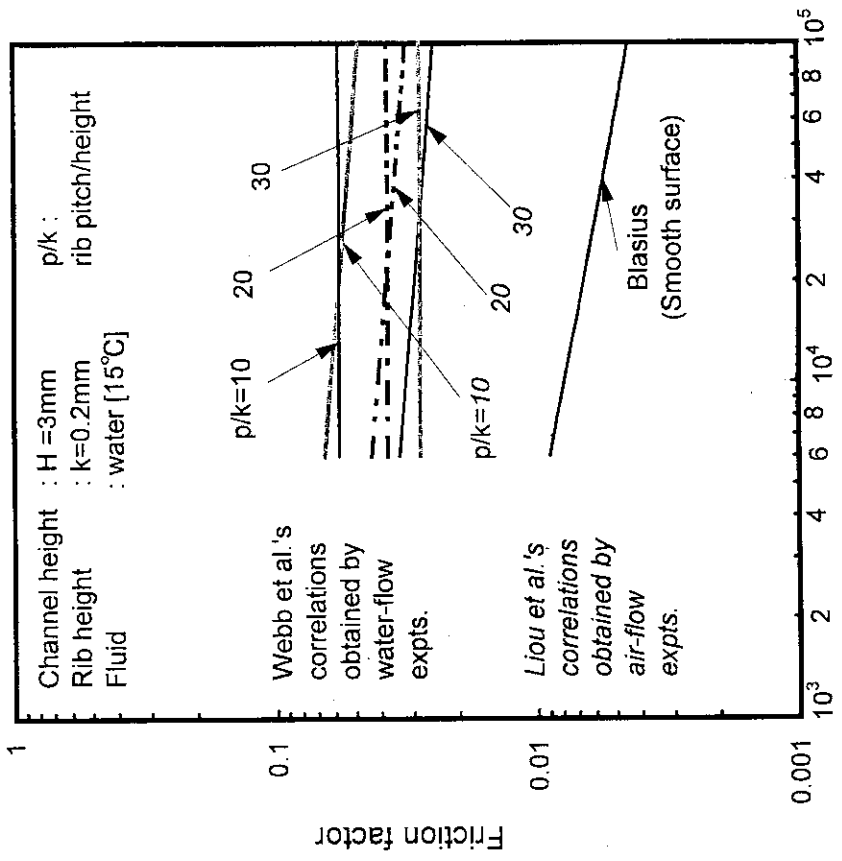

Fig.41 Comparison of Webb et al.'s correlations with Liou et al.'s correlations under water flow condition.

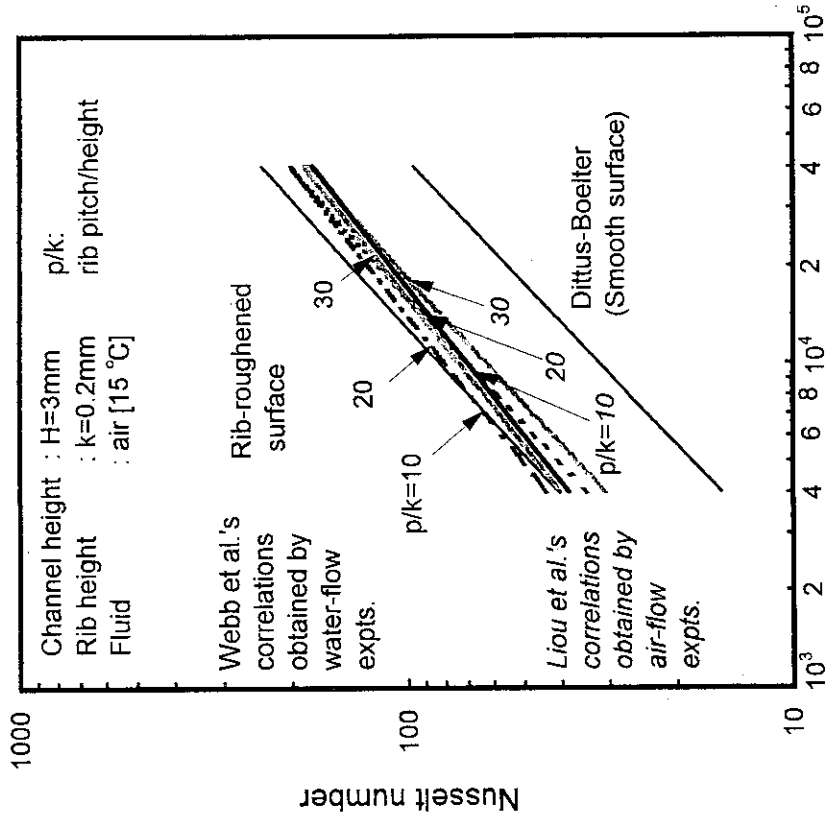

Fig.43 Comparison of Webb et al.'s correlations with Liou et al.'s correlations under air flow condition.

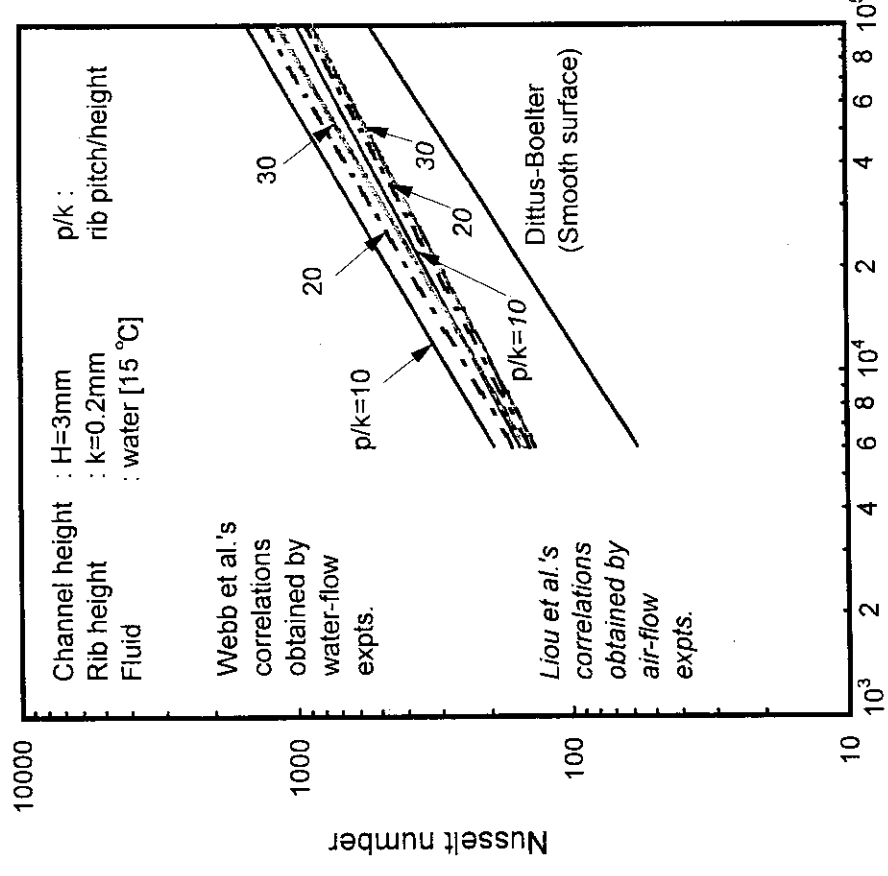

Fig.42 Comparison of Webb et al.'s correlations with Liou et al.'s correlations under water flow condition.

3. Experimental program

Based on the investigation described in chap. 2, an experimental apparatus was proposed to test the augmentation technique and to provide the smooth surface reference data. A schematic diagram of the test apparatus using water as a working fluid is shown in Fig. 44. Only a brief discussion will be addressed here. Water from the pump is supplied to the test section through the flow meter, and then, it passes through a filter, a cooler, a water tank and a pre-heater to the pump. The inlet temperature of the test section is controlled by the pre-heater.

Figure 45 shows the cross section of flow channel and schematic diagram of flow channel with rib-roughened surface. The test section consists of a heating surface made of copper plate with an electric heater, glass windows etc. The cross sectional dimension varies according to channel heights. The width of the test section is 20 mm and channel heights can be varied from 1 mm to 5 mm. Heated length is 200 mm. The rib height and width are 0.2 mm and pitch is 2 mm or 4 mm, respectively. The rib serves as a turbulent promoters to disturb the viscous sublayer of the turbulent boundary layer.

The wall temperatures of the test section are to be measured by 26 copper-constantan thermocouples distributed across the span of the copper plates. Eleven differential pressure taps are installed at opposite side of the heating surface to measure the static pressure drop across the test section. A nichrome plate is used as a heater and receives elcetricity from the DC power supply. The heater provides a constant heat flux for the entire test surface. Three thermocouples of each inlet and outlet of the test section are used to measure the inlet and outlet temperature of water. This type of sophisticated test section will be able to make clear the effectiveness of heat transfer augmentation in a very narrow channel under a wide range of Re region. The proposed experimental conditions are listed in Table 3

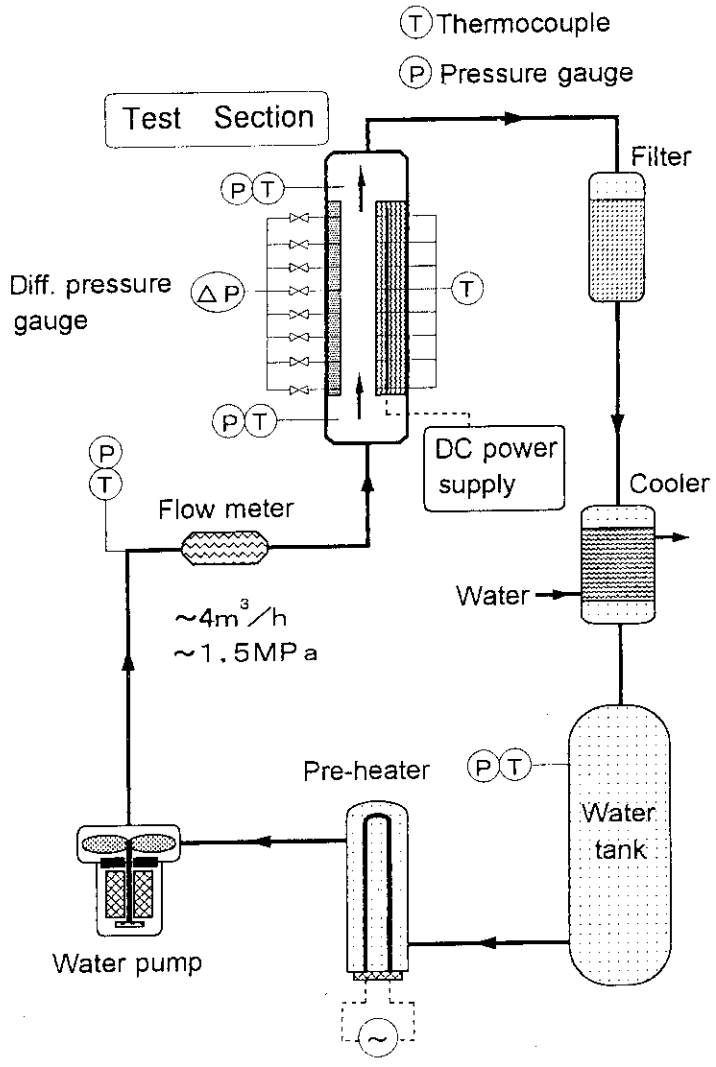

Fig.44 Schematic diagram of test apparatus

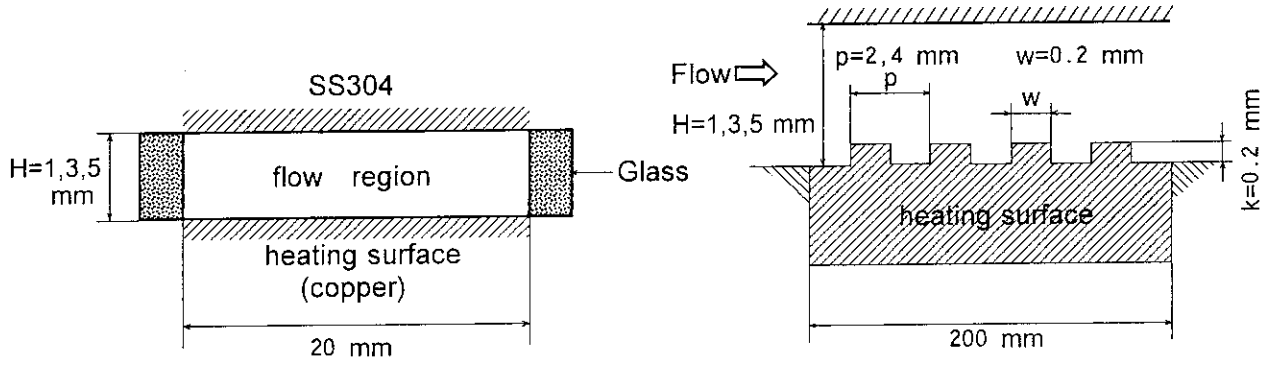

Cross section of flow channel

Flow channel with rib-roughened surface

Fig.45 Schematic drawing of cross section of flow channel and flow channel with rib-roughened surface

4. Concluding Remarks

In the target system, it is needed to remove high heat flux up to 12 MW/m^2 under single-phase forced convection without partial boiling so as to obtain the high intensive neutron generation rate. In order to evaluate coolability of the target system up to such high heat flux, the effect of ribs as turbulent promoters was discussed on the friction factors and heat transfer coefficients for fully developed turbulent flow in very narrow rectangular channels with one-sided rib-roughened constant heat flux condition with different channel heights using previous existing experimental correlations. Webb et al. and Liou and Hwang experimental conditions are cited as for reference data. The following conclusions can be drawn from this analysis.

1. In the case of water-flow, the lower the channel heights, the more heat transfer augmentation can be possible at low velocity (low Re) region. But at higher velocity (high Re) and higher channel heights, the heat transfer augmentation may not be expected.

2. Friction factor of rib-roughened surface is insensitive to the Reynolds number for the case of water-flow and p/k=10 provides the highest friction factor compared to other larger p/k cases. In the case of air-flow, friction factor slightly decreases with increasing of the Reynolds number and p/k=10 also provides the highest friction factor compared to other larger p/k cases.

   For the range of the Reynolds number from 6,000 to 1,00,000, the presence of the square rib at one side and channel height of H=1 mm yields about a 20-39 times, a 10-19 times, and a 7-13 times increase in the friction factor for p/k=10, 20 and 30 respectively, compared to a smooth surface. For channel heights of H=3 and 10 mm, the friction factors of rib-roughened surface are approximately 6-12, 4-7.7, 3.1-5.8 times and 3.3-6.2, 2.4-4.5, 2-3.7 times higher for p/k=10, 20 and 30, compared to the smooth surface.

   In the case of air-flow, the friction factors of rib-roughened surface are approximately 5.3-9.2, 3.4-6.4, 2.6-5.1 times higher than the smooth surface for p/k =10, 20, 30 and the range of the Reynolds number from 1,000 to 40,000. The lowest friction factor is obtained for pitch-to-height ratio (p/k)=30, for both the cases.

3. For the channel height of H=1 mm and water-flow conditions, the pressure drop along the test section is very much high and water velocity will be limited

below 10m/s from the view point of a discharge pressure of a pump installed in the test apparatus. But it is possible to determine the heat transfer coefficients for the smooth and the rib-roughened surfaces up to around 10,000 of the Reynolds number.

4. For the same rib height and spacing, the rib-roughened surface augments heat transfer approximately 3.6-4.3, 2.8-3.3, 2.4-3 times and 2.8-3.4, 2.4-2.9, 2.2-2.6 times higher than the smooth surface when channel heights of H=1 and 3 mm respectively. For channel heights of H=3 and 10 mm, heat transfer augmentation remains almost constant. The rib-roughened surface with p/k=10 provides the highest heat transfer augmentation and largest pressure drop compared to other larger p/k cases.
   In the case of air-flow, for the same rib height and spacing, the rib-roughened surface augments heat transfer approximately 2-2.7, 1.8-2.5, 1.7-2.3 times higher than the smooth surface in channel height of H=1 mm: there is a little effect of channel heights on heat transfer performance. Heat transfer coefficients (Nusselt number) predicted by the correlation obtained by air-flow experiments have large difference from that by water-flow experiments.
5. The incipient boiling temperature of water starts at 182℃ and 151℃ at a pressure of 2 MPa and 1 MPa, respectively. From the surface temperature calculation for the smooth surface, flow boiling will occur at low velocity conditions. For the rib-roughened surface of p/k=10, there is no possibility to occur flow boiling under low velocity conditions down to 1m/s.

On the basis of above results, we proposed an experimental apparatus for further investigation on heat transfer augmentation in a very narrow channel whose configuration will be similar to the cooling passages betwen the target plates under water-flow conditions. The results obtained in this paper have significant implications for the design of coolant channels for the removal of high heat flux from the target plates of a high intensity proton accelerator. The analysis done in this paper is applicable to fully developed turbulent flow in rectangular channels, constant heat flux condition only.

Acknowledgements

In this study, the authors would like to express their sincere gratitude to Mr. Hideki Aita and Mr. Kenji Sekita for assisting how to operate a computer system and how to use software. We appreciate them deeply.

below 10m/s from the view point of a discharge pressure of a pump installed in the test apparatus. But it is possible to determine the heat transfer coefficients for the smooth and the rib-roughened surfaces up to around 10,000 of the Reynolds number.

4. For the same rib height and spacing, the rib-roughened surface augments heat transfer approximately 3.6-4.3, 2.8-3.3, 2.4-3 times and 2.8-3.4, 2.4-2.9, 2.2-2.6 times higher than the smooth surface when channel heights of H=1 and 3 mm respectively. For channel heights of H=3 and 10 mm, heat transfer augmentation remains almost constant. The rib-roughened surface with p/k=10 provides the highest heat transfer augmentation and largest pressure drop compared to other larger p/k cases.
   In the case of air-flow, for the same rib height and spacing, the rib-roughened surface augments heat transfer approximately 2-2.7, 1.8-2.5, 1.7-2.3 times higher than the smooth surface in channel height of H=1 mm: there is a little effect of channel heights on heat transfer performance. Heat transfer coefficients (Nusselt number) predicted by the correlation obtained by air-flow experiments have large difference from that by water-flow experiments.
5. The incipient boiling temperature of water starts at 182℃ and 151℃ at a pressure of 2 MPa and 1 MPa, respectively. From the surface temperature calculation for the smooth surface, flow boiling will occur at low velocity conditions. For the rib-roughened surface of p/k=10, there is no possibility to occur flow boiling under low velocity conditions down to 1m/s.

On the basis of above results, we proposed an experimental apparatus for further investigation on heat transfer augmentation in a very narrow channel whose configuration will be similar to the cooling passages betwen the target plates under water-flow conditions. The results obtained in this paper have significant implications for the design of coolant channels for the removal of high heat flux from the target plates of a high intensity proton accelerator. The analysis done in this paper is applicable to fully developed turbulent flow in rectangular channels, constant heat flux condition only.

Acknowledgements

In this study, the authors would like to express their sincere gratitude to Mr. Hideki Aita and Mr. Kenji Sekita for assisting how to operate a computer system and how to use software. We appreciate them deeply.

References

1.Bejan Adrian, 1989, " Convective Heat Transfer", John Wiley & Sons, New York

2.Berger F.P. and Hau K.-F, F.-L., 1979, "Local Mass / Heat Transfer Distribution on surfaces Roughened with Small Square Ribs" Int. J. Heat Mass Transfer, Vol. 22, pp. 1645 - 1656

3. Carl A. James, B.K. Hodge, and Robert P. Taylor, 1993, " A Discrete Element Method for The Prediction of Friction and Heat Transfer Characteristics of Fully-Developed Turbulent flow in Tubes with Rib-roughness", HTD - Vol. 239, Turbulent Enhanced Heat Transfer ASME 1993

4. Carl A. James, B.K. Hodge, and Robert P. Taylor, 1993, " A Discrete Element Predictive Method for Two-Dimensional Rib Roughness in Fully-Developed Turbulent pipe flow", FED - Vol. 150, Individual papers in Fluids Engineering, ASME 1993

5. Han et al. , 1978, " An Investigation of Heat Transfer and Friction for Rib-Roughened surfaces", Int. J. Heat Mass Transfer, Vol. 21, pp. 1143 - 1156

6. Han et al., 1984, " Heat Transfer and Friction factor in Channels with Two Opposite Rib-Roughened Walls", Transactions of The ASME, Vol. 10 pp.774 - 781

7. Han et al., 1985, " Heat Transfer Enhancement in Channels with Turbulence Promoters", Transactions of The ASME, Vol. 107, pp. 628- 635

8. IPNS Upgrade : A Feasibility Study, ANL-95/13, Argonne National Laboratory, April,1995

9. Liou and Hwang, 1993, " Effect of Ridge Shapes on Turbulent Heat Transfer and Friction in a Rectangular Channel", Int. J. Heat Mass Transfer, Vol. 36, No.4 pp. 931 - 940

10. Liou and Hwang, 1992, " Turbulent Heat Transfer Augmentation and Friction in Periodic fully Developed Channel Flows", Transaction of The ASME, Vol.114, pp. 56 - 64

11. Rohsenow W. M and Hartnett J.P, 1973, " Hand book of Heat Transfer", McGraw-Hill, New York,

12. Swamee, P.K. , and Jain, A.K. , 1976 , " Explicit Equations for Pipe Flow Problembs", Proc. ASCE, J. Hyd. Div. , Vol. 102, Hy5, p.567

13. Webb et al., 1971, " Heat Transfer and Friction in Tubes With Repeated-Rib Roughness", Int. J. Heat Mass Transfer, Vol. 14, pp. 601- 617

14. Zhang Y.M. et al., 1994, " Heat Transfer and Friction in Rectangular Channels with Ribbed or Ribbed-Grooved Walls", Transactions of The ASME, Vol. 116, pp. 58 - 65

Nomenclature

a_1, a_2, a_3	empirical constants
b_1, b_2, b_3	empirical constants
CHF	critical heat flux, W /m^2
C_p	specific heat, J/kg℃
D_e	equivalent diameter, $D_e = 4WH / 2(W+H)$, m
E_r	rib augmentation factor, $E_r = Nu_r / Nu_s$
f	friction factor
G	mass flux, $G = \rho\ u_m$, kg /m^2.s
g	acceleration due to gravity , m/s^2
h	forced convection heat transfer coefficient , W / m^2℃
H	channel height , m
k	rib height , m
K	geometry constant
k^+	roughness Reynolds number, $k^+ = (k/D_e)\ Re\ (f/2)^{1/2}$
L	channel length , m
Nu	Nusselt number, $Nu = hD_e / \lambda$
p	rib spacing , m
P	pressure , N / m^2
Δ P	pressure difference , N / m^2 [refer to eq.(7)]
Pr	Prandtl number, $Pr = C_p\ \mu / \lambda$
q_s	heat flux , W / m^2
R	pipe radius , m

Re	Reynolds number, $Re = D_e u_m / \nu$
St	Stanton number, $St = Nu / Pr\ Re$
T_b	bulk mean temperature, ℃
T_s	saturation temperature , ℃
T_w,	wall temperature , ℃
$\triangle T$	temperature difference, $(T_w - T_b) = D_e q_s / Nu\ \lambda$, ℃
u	local fluid velocity , m/s
u_c	velocity at pipe center line , m/s
u_m	average fluid velocity , m/s
u^*	friction velocity, $u^* = [\tau_o / \rho]^{1/2}$, m/s
u^+	dimensionless velocity, u / u^*
u_k^+	roughness function, [refer to eq. (4)]
w	rib width , m
W	width of the channel , m
x	local distance along the axial direction , m
y	coordinate distance normal to wall , m
y^+	dimensionless distance, $y^+ = y \times u^* / \nu$

Greek symbol

μ	dynamic viscosity , kg/m.s
ν	kinematic viscosity , m^2/s
ρ	density , kg/m^3
τ	local shear stress , N/m^2
τ_o	apparent wall shear stress, $\tau_o = D_e \times \triangle P / 4L$, N/m^2
σ_l	viscous sublayer thickness , $\sigma_l = 5 \times \nu / u^*$, m
σ_b	buffer layer thickness, $\sigma_b = 40 \times \nu / u^*$, m
λ	thermal conductivity , W/m℃

Subscripts

b	bulk
i	incipient boiling
m	mean
r	rib-roughened surface
s	smooth surface
w	wall